

Requirement falsification for cyber-physical systems using generative models

Jarkko Peltomäki* and Ivan Porres
 Faculty of Science and Engineering,
 Åbo Akademi University
 Turku, Finland
 name.surname@abo.fi

Abstract

We present the OGAN algorithm for automatic requirement falsification of cyber-physical systems. System inputs and output are represented as piecewise constant signals over time while requirements are expressed in signal temporal logic. OGAN can find inputs that are counterexamples for the safety of a system revealing design, software, or hardware defects before the system is taken into operation. The OGAN algorithm works by training a generative machine learning model to produce such counterexamples. It executes tests atomically and does not require any previous model of the system under test. We evaluate OGAN using the ARCH-COMP benchmark problems, and the experimental results show that generative models are a viable method for requirement falsification. OGAN can be applied to new systems with little effort, has few requirements for the system under test, and exhibits state-of-the-art CPS falsification efficiency and effectiveness.

1 Introduction

Cyber-physical systems (CPS) [41] integrate complex hardware and software components to interact autonomously with their physical environment in real time. Examples of CPS range from smart home systems to autonomous vehicles. Most CPS are considered safety-critical systems since they may cause injuries, environmental damage, or economical losses if they fail. It is therefore paramount to assess the safety of a CPS before it is taken into operation. This requires rigorous verification and validation methods to identify and remove potential defects.

In this article, we present a novel method for safety validation by requirement falsification [7]. Requirement falsification is a method based on the search for system inputs that yield outputs that violate a given system requirement. It can be understood as a form of runtime verification, i.e., search-based test design and execution guided by formal requirements [5]. Due to the real-time nature of CPS, execution traces are usually represented as signals over time, and requirements are expressed using signal temporal logic (STL) [31]. A requirement falsification algorithm iteratively generates a system input, executes it on the system under test (SUT), observes the system output with a runtime monitor, and evaluates if the requirement is satisfied or not. If the algorithm finds an input for which the given requirement is not satisfied, then that input is a counterexample against the claim that the system is safe with respect to the requirement.

Requirement falsification can be automated by formulating it as an optimization problem where a robustness metric is minimized [16, Sec. 3.2]. A robustness metric is a function from an execution trace (a pair of system inputs and outputs) to a single real value. The convention is that a robustness metric has the following two properties. First, it is negative if the trace does not satisfy the requirement. Second, if the requirement is satisfied, then the robustness is positive

*Corresponding author.

and indicates how close the trace is from being falsifying. These properties can be used together with a minimization algorithm to search for inputs that do not satisfy a given requirement.

The main benefits of requirement falsification via a robustness metric are that it can be fully automated and that it is a black-box method. The latter implies applicability to any system or model of a system as long as it is executable and its inputs and outputs are observable. The main drawback is that, given a limited testing budget, requirement falsification is sound as a verification method, but it is not complete, i.e., it can miss faults. Therefore, research on requirement falsification focuses on algorithms that can find faults effectively and efficiently within a limited testing budget. The presence of a limited budget is motivated by the cost to execute each test.

In this article, we present a new algorithm for requirement falsification based on learning two models: one that serves as a surrogate of the composition of the SUT and the robustness metric and another that serves as a query strategy for the surrogate model. The latter model is a generative model, the *generator*, and it generates system inputs from random noise. The surrogate model, called the *discriminator*, predicts the robustness of system inputs. We implement both models as neural networks and train them in a fashion inspired by Generative Adversarial Networks (GAN) [21]. The algorithm is generic since it applies to any black-box SUT with requirements specified in STL. Moreover, the models are trained online without the need for a previous dataset for the SUT. We call the algorithm OGAN for online generative adversarial network.

There are two important design decisions for requirement falsification algorithms that can affect their applicability and performance. The first is whether or not testing is considered to be an atomic operation, and the second is whether or not knowledge collected before the start of the falsification task can be used. The precollected knowledge can include surrogate models, handcrafted system monitors, or highly customized hyperparameters.

A test is executed atomically if the input signals must be provided completely before the test execution can start. In contrast, a requirement falsification algorithm using nonatomic testing can interact with the SUT while the test executes and generate the input signals incrementally using not only the information collected from the previous tests but also from the current one. This is not possible when using atomic test execution.

The OGAN algorithm uses atomic testing. The reason is that nonatomic testing may not be feasible in practice since it imposes real-time constraints on the falsification algorithm. This is the case when the SUT has strict real-time requirements, e.g., due to hardware-in-the-loop subsystems. The fact that OGAN uses atomic testing makes it more generic: it can be applied to any SUT.

To simplify its application to new problems, OGAN does not require the use of previously trained models or custom monitors. Although such artifacts can help in falsification, it is hard to assess the computational and human effort required to create them. OGAN learns its models tabula rasa, and the effort to do that is included in the effort required for the falsification task.

We evaluate the effectiveness and efficiency of OGAN experimentally on benchmarks derived from the falsification track of the ARCH-COMP competition [13, 14, 33], which is a friendly research competition on the verification of continuous and hybrid systems. We present evidence that OGAN’s effectiveness and efficiency are on par with the state-of-the-art requirement falsification algorithms of the ARCH-COMP competition.

The OGAN algorithm has been used previously in the context of performance testing [40] and the falsification of multiple requirements in combination with multi-armed bandits [37]. In this work, we provide for the first time a complete description of OGAN including all necessary theoretical considerations. Moreover, we discuss the practical implementation of OGAN as a part of a falsification tool. The main contributions of the article are as follows.

- A requirement falsification algorithm based on generative models that uses atomic testing, supports arbitrary STL requirements, and does not require any previous model or data. The hyperparameter setup of the described implementation provides competitive results on a wide range of problems.
- A scaled robustness metric for STL. This is proposed to improve the representation of STL robustness in the neural network models used by OGAN.

- A novel methodology to compare the effectiveness and efficiency of requirement falsification algorithms based on survival analysis.
- A comprehensive evaluation of the OGAN algorithm. This includes evaluating the accuracy of the discriminator model and the generator Monte Carlo sampling strategy.

We proceed as follows. Section 2 describes the problem of requirement falsification and presents the overall ideas on how to use generative machine learning to solve it. We present the OGAN algorithm as a concrete realization of these ideas in Section 3. Section 4 presents the syntax and semantics of STL and how to automatically obtain scaled robustness metrics for STL requirements. We then proceed to the evaluation of OGAN. The main research questions and the methodology to answer them are found in Section 5 while the actual experimental results are discussed in Section 6. We conclude by presenting related work (Section 7) and conclusions (Section 8).

2 Requirement Falsification Using Generative Models

2.1 System Under Test

We represent the system under test (SUT) as a deterministic function \mathcal{M} from an input space \mathcal{I} to an output space \mathcal{O} . We assume that the spaces \mathcal{I} and \mathcal{O} are either compact subsets of a Euclidean vector space or function spaces containing signals $[0, T] \rightarrow \mathbb{R}^n$ for some $T > 0$. For the convenience of discussion, we represent vector inputs as constant signals.

For example, the inputs in the AT1₂₀ benchmark of Subsection 5.3 are a vehicle’s throttle and brake signals over a time interval of 30s taking values respectively in $[0, 100]$ and $[0, 325]$. In the F16 benchmark, the input is a vector of length three representing the initial roll, pitch, and yaw of an aircraft. The output signal is the altitude of the aircraft during its 15s maneuver.

We remark that in practice continuous signals need to be discretized appropriately, and a high enough sampling rate needs to be used so that violations and non-violations of the requirements can be meaningfully detected. In this article, we sample the input signals evenly every 0.01 seconds.

2.2 Falsification of Formal Requirements

Let $\mathcal{M}: \mathcal{I} \rightarrow \mathcal{O}$ be a SUT. Falsifying a requirement represented as a formula φ means producing an input (a test) x in \mathcal{I} such that the behavior of the SUT for x violates φ . More precisely,

$$\varphi \text{ is falsified for the input } x \text{ if } (\mathcal{M}(x), 0) \not\models \varphi$$

where $(\mathcal{M}(x), 0) \not\models \varphi$ means that the signal $\mathcal{M}(x)$ does not satisfy φ when evaluated at time 0. We abuse notation and consider $\mathcal{M}(x)$ to contain both output and input signals, that is, $\mathcal{M}(x)$ is the execution trace. This is needed as a requirement might involve both inputs and outputs. We evaluate the truth value at time 0 simply for convenience, and the discussion is easily adjusted to cover a more general setting. In what follows, we focus only on falsifying a single requirement.

2.3 Robustness-Based Falsification

Our central assumption is that the SUT is a black-box function meaning that we cannot solve for falsifying inputs, and all we can do is to search for them. We assume that associated to a requirement φ , there is a *robustness metric* ρ taking values in \mathbb{R} . A robustness metric has the properties that if $\rho(\mathcal{M}(x)) > 0$ then $(\mathcal{M}(x), 0) \models \varphi$ and if $\rho(\mathcal{M}(x)) < 0$ then $(\mathcal{M}(x), 0) \not\models \varphi$. Moreover, we informally specify ρ to have the following property: the smaller the values of $\rho(\mathcal{M}(x))$ are, the closer the input x is to falsifying φ . This property will be made precise in Subsection 4.1 when we introduce the STL robustness metric. The case $\rho(\mathcal{M}(x)) = 0$ is often ambiguous, and we ignore it here; see the discussion in Subsection 4.1.

The above properties are ideal for searching falsifying inputs: falsifying φ amounts to minimizing ρ . In other words, the falsification of φ reduces to solving the following optimization problem:

$$\arg \min_{x \in \mathcal{I}} \rho(\mathcal{M}(x)). \quad (1)$$

In fact, solving for the global minimum is often unnecessary, and we simply want to show that there exists x in \mathcal{I} such that $\rho(\mathcal{M}(x)) < 0$.

The success of this approach depends on how complicated the function ρ is. It is not true in general that the function $x \mapsto \rho(\mathcal{M}(x))$ is smooth or even continuous everywhere. It is reasonable to assume that it is, for example, locally Lipschitz continuous. The validity of this assumption depends on the SUT, the requirement, and the robustness metric. We remark that the robustness metric employed in this paper is quite well-behaved when viewed as a function $\mathcal{O} \rightarrow \mathbb{R}$. Moreover, in our experiments, the SUT’s inputs are piecewise constant and the outputs are rather regular.

Notice that solving (1) relying solely on the robustness metric ρ means that test execution is, for all practical purposes, atomic. Indeed, without knowing the trace $\mathcal{M}(x)$ completely, it might not be possible to compute $\rho(\mathcal{M}(x))$. Thus if the optimization is to use partial traces effectively, estimating and bounding the robustness metric based on partial traces is required. We do not explore nonatomic test execution in this article, so we do not discuss this matter further. We remark that lower and upper bounds for a robustness metric have been considered, e.g., in [12].

2.4 Robustness-Based Falsification Using Generative Models

Next we describe our idea how to perform robustness-based falsification of a requirement using generative machine learning.

First, we discuss normalized representation of inputs and outputs. This is needed as machine learning models require inputs and outputs to be given in explicit form. More importantly, it is often recommended to normalize the inputs of machine learning models as it improves convergence. Indeed, in the particular case of neural networks, with constant-sign inputs and activation functions, the convergence, while not impossible, can be very slow [30]. For us convergence is especially important as the training data is obtained on the fly and new training data is collected using models trained with little data. An additional benefit of normalization is that the generative models can be agnostic about the actual ranges of the system inputs and outputs.

Consider a SUT \mathcal{M} , a requirement φ , and an associated robustness metric ρ . We represent the input space \mathcal{I} as the set $[-1, 1]^D$ for some D . We assume that there is an implicit mechanism that maps this set injectively to the actual input space of the SUT. For the experiments of this paper, we explain the mechanism in Subsection 5.4. Likewise, we assume that there is a *scaled robustness metric*: a function $\bar{\rho}$ that maps the values $\rho(\mathcal{M}(x))$ to the interval $[0, 1]$ with the interpretation that if $\bar{\rho}(\mathcal{M}(x)) > 0$ then $(\mathcal{M}(x), 0) \models \varphi$. Again we require informally that the smaller the values of $\bar{\rho}(\mathcal{M}(x))$ are, the closer the input x is to falsifying φ . This is important so that the falsification task can be transformed into an optimization problem as described in Subsection 2.3. The scaled robustness function used in the experiments of this paper is described in Subsection 4.2. Notice that our assumptions are rather mild. Our ideas are thus general and apply to a wide variety of systems and requirements.

Let us now return to the main topic of falsification using generative models. Let \mathcal{H} denote a latent space $[-1, 1]^L$ for some L . Let \mathcal{F} be the set of failing tests, that is, let

$$\mathcal{F} = \{x \in \mathcal{I} : \bar{\rho}(\mathcal{M}(x)) = 0\}.$$

The problem we would like to solve is the problem of training a generator $\mathcal{G}: \mathcal{H} \rightarrow \mathcal{I}$ which maps the uniform distribution on \mathcal{H} to the uniform distribution supported on \mathcal{F} . Here we focus on the more practical goal of training the generator so that

$$\mathcal{G}(\mathcal{H}) \subseteq \{x \in \mathcal{I} : \bar{\rho}(\mathcal{M}(x)) < \varepsilon\} \quad (2)$$

for a small ε . Given such a generator, system inputs with low robustness can be sampled by sampling the uniform distribution on \mathcal{H} and mapping the samples through \mathcal{G} .

In order to train the generator, we introduce a *discriminator*¹ $\mathcal{D}: \mathcal{I} \rightarrow [0, 1]$ which we train to learn the mapping $x \mapsto \bar{\rho}(\mathcal{M}(x))$, $x \in \mathcal{I}$. As stated above, the aim is to train \mathcal{G} so that $\bar{\rho}(\mathcal{M}(\mathcal{G}(y))) < \varepsilon$ for all $y \in \mathcal{H}$, so we use \mathcal{D} as a proxy for ρ and train \mathcal{G} on \mathcal{D} by minimizing

$$\frac{1}{|\mathcal{B}|} \sum_{y \in \mathcal{B}} \mathcal{L}(\mathcal{D}(\mathcal{G}(y)), 0) \quad (3)$$

for a loss function \mathcal{L} and a batch \mathcal{B} of elements sampled from \mathcal{H} .

The main unaddressed issue so far is how to obtain or train the discriminator \mathcal{D} . Because we wish to avoid using any precollected data or pretrained models, the only option is to train \mathcal{D} online. We propose to approach this as follows. First, we obtain an initial training data. This can be done by uniform random sampling or a similar Monte-Carlo method. Based on this initial data, the discriminator \mathcal{D} can be trained and consequently the generator \mathcal{G} can be trained against it as proposed above. In practice, it is unlikely that this yields a good generator especially if the initial training data is small or contains few tests with low robustness. It is therefore crucial to augment the discriminator’s training data. For the augmentation, there are essentially two approaches: 1) continue the Monte-Carlo sampling, 2) sample the generator \mathcal{G} for tests. These two options can be even combined by alternating between them.

Let us then discuss the latter approach of using \mathcal{G} for training data augmentation. Once \mathcal{G} has been trained against \mathcal{D} , we can sample \mathcal{G} for tests by sampling the uniform distribution on the latent space as described above. Let x be such a test. The test x can be executed on the SUT to learn $\mathcal{M}(x)$. If $\bar{\rho}(\mathcal{M}(x)) < \varepsilon$, then \mathcal{G} has successfully performed its job. If the same result is obtained for several other sampled tests, we can consider that the required generator has been found. If this is not the case, we can, in principle, improve the discriminator’s accuracy by introducing pairs $(x, \bar{\rho}(\mathcal{M}(x)))$ into its training data. The generator \mathcal{G} can then be retrained on the improved discriminator, and the process can be repeated.

Intuitively, the process described above eventually leads to finding a generator \mathcal{G} that satisfies (2). In practice, the process can get stuck due to local minima. However, we may still be able to sample at least one element from \mathcal{F} during the training. This suffices for falsification.

Above, we focused on using the partially trained generator as a mechanism to obtain more training data for the discriminator. As stated previously, this can also be done using Monte-Carlo sampling. However, we expect that using the generator is more efficient. An input sampled from \mathcal{G} with high robustness provides \mathcal{D} immediate feedback about its inaccuracies whereas a test obtained via Monte-Carlo sampling can be unhelpful in improving \mathcal{D} .

3 The OGAN Algorithm

In this section, we present the OGAN algorithm for robustness-based requirement falsification using generative models. It is founded on ideas presented in Subsection 2.4.

In the previous section, we did not give any stopping condition for the training of the generator. Below we have chosen to use an execution budget as such a condition. This is natural as we assume that evaluating the SUT (i.e, executing a test) is expensive. We have not designed any mechanism to assess generator quality during the algorithm execution. The experimental evaluation of Section 6 indicates that the quality is good enough for falsification purposes.

We have decided to model the generator \mathcal{G} and the discriminator \mathcal{D} as neural networks. This is important as it allows \mathcal{G} to be trained against \mathcal{D} by freezing the weights of \mathcal{D} and applying the usual back-propagation of errors to the weights of \mathcal{G} . Thus \mathcal{G} is a neural network mapping \mathbb{R}^L (the latent space) to \mathbb{R}^D (the input space), and \mathcal{D} maps \mathbb{R}^D to \mathbb{R} . The inputs are always given as

¹The word discriminator is used here because our research is inspired by generative adversarial networks. The discriminator defined here does not play the same role as discriminators in generative adversarial networks.

Algorithm 1 OGAN requirement falsification algorithm.

Require: SUT \mathcal{M} , execution budget E , number N of tests to be sampled initially, sampling probability P , batch size B , discriminator training epochs $E_{\mathcal{D}}$, generator training epochs $E_{\mathcal{G}}$, multiplier α .

```

1:  $T \leftarrow \text{SAMPLE}(\mathcal{I}; N)$ 
2:  $F \leftarrow \text{EXECUTE}(\mathcal{M}; T)$ 
3: while  $|T| < E$  do
4:    $\mathcal{G}, \mathcal{D} \leftarrow \text{INITIALIZE\_OGAN\_MODELS}()$ 
5:   for  $i \in \{1, \dots, E_{\mathcal{D}}\}$  do
6:      $\text{TRAIN\_DISCRIMINATOR}(\mathcal{D}; T, F)$ 
7:   for  $i \in \{1, \dots, E_{\mathcal{G}}\}$  do
8:      $X \leftarrow \text{SAMPLE}(\mathcal{H}; B)$ 
9:      $\text{TRAIN\_GENERATOR}(\mathcal{G}; \mathcal{D}(\mathcal{G}(X)), 0)$ 
10:   $\text{test} \leftarrow \text{SAMPLE\_TEST}(\mathcal{G}, \mathcal{D}; P)$ 
11:   $\text{test\_robustness} \leftarrow \text{EXECUTE}(\mathcal{M}; \text{test})$ 
12:   $T \leftarrow T \cup \{\text{test}\}$ 
13:   $F \leftarrow F \cup \{\text{test\_robustness}\}$ 

14: function  $\text{SAMPLE\_TEST}(\mathcal{G}, \mathcal{D}; P)$ 
15:   if  $\text{RANDOM}() \leq P$  then
16:      $\text{test} \leftarrow \text{SAMPLE}(\mathcal{I}; 1)$ 
17:   else
18:      $Q \leftarrow \text{INITIALIZE\_PRIORITY\_QUEUE}()$ 
19:      $\text{accept\_threshold} \leftarrow 0$ 
20:     repeat
21:        $\text{candidate\_test} \leftarrow \text{SAMPLE}(\mathcal{G}; 1)$ 
22:        $\text{estimated\_robustness} \leftarrow \text{ESTIMATE\_ROBUSTNESS}(\mathcal{D}; \text{candidate\_test})$ 
23:        $\text{ADD\_TO\_QUEUE}(Q; \text{estimated\_robustness}, \text{candidate\_test})$ 
24:        $\text{accept\_threshold} \leftarrow 1 - \alpha \cdot (1 - \text{accept\_threshold})$ 
25:     until  $\text{MIN}(Q) \leq \text{accept\_threshold}$ 
26:      $\text{test} \leftarrow \text{TEST\_WITH\_MIN\_ROBUSTNESS}(Q)$ 
27:   return  $\text{test}$ 

```

elements of $[-1, 1]^K$ and $[-1, 1]^D$, and an appropriate activation function is used to ensure that the ranges of \mathcal{G} and \mathcal{D} are respectively contained in $[-1, 1]^D$ and $[0, 1]$.

The pseudo code for our proposal to implement the ideas of Subsection 2.4 is given in Algorithm 1. The code omits many practical details like the neural network structure and the loss function. These choices are made concrete in Subsection 5.4 where the setup for our evaluation of OGAN is described.

Let us describe the pseudo code in detail. On line 1, the test suite T is populated by a sample of size N via the chosen Monte-Carlo sampling algorithm. For example, uniform random sampling on $[-1, 1]^D$ can be used for this purpose. Line 2 executes the tests on the SUT, and saves the corresponding scaled robustness function values into the structure F (OGAN uses the SUT output only to compute the robustness). Line 3 begins the main loop of the algorithm, and its execution resumes until the execution budget (number of allowed executions) has been exhausted. On lines 4–9, the models \mathcal{G} and \mathcal{D} are initialized and trained. The model \mathcal{D} is trained using the training data (T, F) collected so far for a certain amount of training epochs $E_{\mathcal{D}}$. Lines 8–9 correspond to training \mathcal{G} against \mathcal{D} , as in (3), for a certain number of epochs $E_{\mathcal{G}}$. On lines 10–13, a new test is sampled, executed, and it and its robustness are added to the discriminator’s training data. After the algorithm has executed, the test suite T can be inspected for falsifying tests.

Let us next look at the sampling of a new test, i.e., the function on line 14. This function

samples a new test via Monte-Carlo sampling with probability P ; otherwise \mathcal{G} is sampled (see below). The reason for this is the following. If the falsification of the requirement is of unknown difficulty, then it is not obvious how to set the initial random sampling budget N . If the problem is easy, then a small N should suffice for OGAN to falsify, and setting N too large can use an excessive amount of executions before a falsification is observed. If the problem is not easy, then a larger N can help the discriminator to learn the mapping better globally. Monte-Carlo sampling with probability P after the initial phase allows to set the number N to be small: tests independent of the generator will be executed throughout the whole execution of the algorithm. This probability P thus strikes a balance between exploration and exploitation. More sophisticated sampling strategies based on, e.g., multi-armed bandits, could be used here, but we have not explored this.

Let us finally describe the test sampling using \mathcal{G} , which corresponds to lines 18–26 of Algorithm 1. The loop starting on line 20 first samples \mathcal{G} (i.e., samples the uniform distribution on \mathcal{H} and maps the samples via \mathcal{G}) for a test. Then it estimates its robustness using \mathcal{D} . This is a crucial step as this avoids expensive execution of tests on the SUT. If the estimated robustness is low enough, then the test is accepted and returned. We sample many tests and check them against an acceptance threshold because, due to the random nature of the sampling, we are not guaranteed to immediately sample a test with the lowest possible estimated robustness. The acceptance threshold is progressively increased on each round of the loop because i) we want to accept tests reasonably fast, ii) the estimates of \mathcal{D} might have a large lower bound. The threshold increases from 0 to 1 like 1 decreases to 0 when repeatedly multiplied by the number α . We use a priority queue Q to select the candidate with the lowest estimated robustness.

As explained in Subsection 2.4, we expect that a falsifying test is executed on the SUT during the execution of OGAN. We do not have any theoretical guarantees for this, but the evaluation of OGAN presented in Section 6 shows that this happens in practice.

4 Requirements in Signal Temporal Logic

The requirements for the benchmarks selected for the evaluation of the OGAN algorithm (see Section 6) are expressed in signal temporal logic (STL) [31]. In this section, we completely describe STL syntax and semantics and show how to transform an STL requirement into a robustness metric. The main contribution of this section is in Subsection 4.2, which describes how to transform an STL robustness metric into a scaled robustness metric as required in Subsection 2.4.

The requirements we consider here are STL formulas φ whose predicates refer to the inputs and outputs of a SUT. For example, if the SUT outputs a signal $\text{SPEED}: [0, 30] \rightarrow [0, \infty)$, then the formula

$$\Box_{t \in [0, 20]} \text{SPEED}(t) < 120$$

expresses that the output signal should never exceed 120 during the first 20 time units.

A precise definition of STL follows. Let \mathbb{T} be a discrete time domain, that is, $\mathbb{T} = [A, B] \cap \mathbb{Z}$ with $A, B \in \mathbb{Z}$ and $A < B$. In what follows, we simply write $[A, B]$ for $[A, B] \cap \mathbb{Z}$. A signal s is a function $s: \mathbb{T} \rightarrow \mathbb{R}$. For convenience, we represent several signals with a common time domain as a single vector-valued signal \mathbf{s} . Let $P = \{p_1, \dots, p_n\}$ be a set of predicates $p_i: \mathbb{T} \rightarrow \{\top, \perp\}$, $i = 1, \dots, n$, whose truth value depends on both time t and a signal \mathbf{s}_i . The grammar of the *signal temporal logic* (STL) is defined recursively by

$$\varphi := p \mid \neg\varphi \mid \varphi \wedge \psi \mid \varphi \mathcal{U}_{\mathcal{I}} \psi$$

where φ, ψ are STL formulas, $p \in P$, and \mathcal{I} is an interval in \mathbb{T} (open, closed, or half-open). As is usual, we let $\varphi \vee \psi$ be shorthand for $\neg(\neg\varphi \wedge \neg\psi)$ and $\varphi \rightarrow \psi$ for $\neg\varphi \vee \psi$. In addition, we define the temporal operators *eventually* $\Diamond_{\mathcal{I}}\varphi := \top \mathcal{U}_{\mathcal{I}}\varphi$ (here \top is a predicate which always evaluates to true) and *always* $\Box_{\mathcal{I}}\varphi := \neg\Diamond_{\mathcal{I}}\neg\varphi$. The operator $\mathcal{U}_{\mathcal{I}}$ is called the *until* operator.

We write $(\mathbf{s}, t) \models \varphi$ to indicate that a signal \mathbf{s} satisfies the formula φ at time t . This relation is defined inductively as follows:

$$\begin{aligned} (\mathbf{s}, t) \models p_{i, \mathbf{s}_i} &\iff p_{i, \mathbf{s}_i}(t) = \top, \\ (\mathbf{s}, t) \models \neg\varphi &\iff (\mathbf{s}, t) \not\models \varphi, \\ (\mathbf{s}, t) \models \varphi \wedge \psi &\iff (\mathbf{s}, t) \models \varphi \text{ and } (\mathbf{s}, t) \models \psi, \quad \text{and} \\ (\mathbf{s}, t) \models \varphi \mathcal{U}_{\mathcal{I}} \psi &\iff \exists t' \in t + \mathcal{I}: (\mathbf{s}, t') \models \varphi \quad \forall t'' \in [t, t'] \text{ and } (\mathbf{s}, t'') \models \psi. \end{aligned}$$

The interpretation for the until operator is that the formula φ evaluates to true until the formula ψ evaluates to true. Notice that φ needs to evaluate to true from the time point t which might be outside of $t + \mathcal{I}$. The interpretations of the remaining operators are obvious.

It follows from above that

$$\begin{aligned} (\mathbf{s}, t) \models \diamond_{\mathcal{I}}\varphi &\iff \exists t' \in t + \mathcal{I}: (\mathbf{s}, t') \models \varphi \quad \text{and} \\ (\mathbf{s}, t) \models \square_{\mathcal{I}}\varphi &\iff \forall t' \in t + \mathcal{I}: (\mathbf{s}, t') \models \varphi. \end{aligned}$$

Above, we silently assume that the signal \mathbf{s} is long enough so that it makes sense to talk about the signal value at a time t , that is, we assume that $t + \mathcal{I} \subseteq \mathbb{T}$.

4.1 Traditional STL Robustness Metric

Our next aim is to transform an STL formula φ into a real-valued function ρ such that the following implications are satisfied:

$$\begin{aligned} \rho(\varphi; \mathbf{s}, t) > 0 &\implies (\mathbf{s}, t) \models \varphi \implies \rho(\varphi; \mathbf{s}, t) \geq 0, \\ \rho(\varphi; \mathbf{s}, t) < 0 &\implies (\mathbf{s}, t) \not\models \varphi \implies \rho(\varphi; \mathbf{s}, t) \leq 0. \end{aligned}$$

In other words, the sign of $\rho(\varphi; \mathbf{s}, t)$ determines the truth value of φ whenever $\rho(\varphi; \mathbf{s}, t) \neq 0$. There are infinitely many ways to accomplish this, but we focus here on what we call the traditional robustness metric [11]. Other alternative STL robustness metrics can be found in [44, 19, 48].

First of all, we assume that a robustness metric ρ is given when $\varphi = p$ for a predicate p . In our applications, the predicates take the form of a simple inequality like $\text{SPEED}(t) \leq 120$. We set

$$\rho(X \geq Y; \mathbf{s}, t) = \rho(X; \mathbf{s}, t) - \rho(Y; \mathbf{s}, t),$$

and we let

$$\rho(v; \mathbf{s}, t) = v(t)$$

whenever v refers to a component of \mathbf{s} . We interpret constants in the inequalities as signals with constant value. Our approach cannot distinguish the predicates $X \geq Y$ and $X > Y$ in the case of equality. In order to work around this, we can set $\rho(X \geq Y)$ to be a nonzero constant with appropriate sign in the case of equality. When X and Y refer to continuous quantities, the problem with the value 0 does not often matter in practice. If $X = Y$, then the requirements $X > Y$ and $X \geq Y$ are almost falsified as even the tiniest perturbation of the signals leads to falsification. It is thus natural to count both requirements as falsified.

The robustness metric for more complex STL formulas are found as follows:

$$\begin{aligned} \rho(\neg\varphi; \mathbf{s}, t) &= -\rho(\varphi; \mathbf{s}, t), \\ \rho(\varphi \wedge \psi; \mathbf{s}, t) &= \min\{\rho(\varphi; \mathbf{s}, t), \rho(\psi; \mathbf{s}, t)\}, \quad \text{and} \\ \rho(\varphi \mathcal{U}_{\mathcal{I}} \psi; \mathbf{s}, t) &= \max_{t' \in t + \mathcal{I}} \left(\min \left\{ \rho(\psi; \mathbf{s}, t'), \min_{t'' \in [t, t']} \rho(\varphi; \mathbf{s}, t'') \right\} \right). \end{aligned} \tag{4}$$

From this, we deduce that

$$\begin{aligned}\rho(\diamond_{\mathcal{I}}\varphi; \mathbf{s}, t) &= \max_{t' \in t+\mathcal{I}} \rho(\varphi; \mathbf{s}, t') \quad \text{and} \\ \rho(\square_{\mathcal{I}}\varphi; \mathbf{s}, t) &= \min_{t' \in t+\mathcal{I}} \rho(\varphi; \mathbf{s}, t').\end{aligned}$$

Notice that given φ , \mathbf{s} , and t , the function ρ can be efficiently computed.

It is straightforward to verify that the robustness metric is computed as follows when $\varphi = \square_{t \in [0, 20]} \text{SPEED}(t) < 120$:

$$\rho(\varphi; \text{SPEED}, t) = \min_{t' \in [t, t+20]} (120 - \text{SPEED}(t')).$$

It is an easy exercise to prove that $(\mathbf{s}, t) \models \varphi$ implies that $\rho(\varphi; \mathbf{s}, t) \geq 0$ (whenever the robustness of the predicates satisfies this property as well) and conversely that $\rho(\varphi; \mathbf{s}, t) > 0$ implies that $(\mathbf{s}, t) \models \varphi$ [11, 17]. Analogous statements apply for the opposite-signed statements. Moreover, it is straightforward to see that the following result is true (see [17, Sect. 3.4]).

Lemma 4.1. Let $\pi_i(\mathbf{v})$ be the projection of a vector \mathbf{v} to its i th coordinate. If $\rho(\varphi; \mathbf{s}, t) = \varepsilon$ and \mathbf{s}' is a signal such that $|\pi_i(\mathbf{s}) - \pi_i(\mathbf{s}')| < |\varepsilon|$ for all i , then $(\mathbf{s}, t) \models \varphi$ if and only if $(\mathbf{s}', t) \models \varphi$ given that this property is true for predicates.

The preceding lemma shows why the name robustness metric was chosen: if $\rho(\varphi; \mathbf{s}, t)$ is large in absolute value, then the truth value is robust to large changes in the signal \mathbf{s} .

4.2 Scaling the Traditional STL Robustness Metric

In this section, we investigate the effective range of an STL formula φ and define a scaled robustness metric $\bar{\rho}$ based on it. This metric takes values in $[0, 1]$ with the interpretation that 0 corresponds to falsification. In particular, we can let the objective for the optimization problem (1) to be $\bar{\rho}(\varphi; \mathbf{s}(x), 0)$ where $\mathbf{s}(x)$ is a vector-valued signal whose components include the input x and output $\mathcal{M}(x)$ of the SUT (recall that we evaluate robustness metrics at time $t = 0$ by convention).

The motivation for scaling the robustness metric is to improve convergence as discussed in Subsection 2.4. The proposed scaling method is slightly complicated, and we propose it to overcome some problems in naive scaling; see Subsection 4.2.2 for further details.

4.2.1 Effective Range of an STL Formula

In this section, we study how to scale the traditional robustness metric ρ . If \mathcal{I} is an interval, then we denote respectively by \mathcal{I}^- and \mathcal{I}^+ its left and right endpoints.

In what follows, we define the *effective range* $\mathcal{I}(\varphi; \mathbf{s}, t)$ of an STL formula φ for a signal \mathbf{s} at time t . Once such a range is defined, we obtain a *scaled robustness metric* $\bar{\rho}$, taking values in $[0, 1]$, by setting

$$\bar{\rho}(\varphi; \mathbf{s}, t) = \begin{cases} 0, & \text{if } \rho(\varphi; \mathbf{s}, t) \leq 0, \\ \rho(\varphi; \mathbf{s}, t) / \mathcal{I}^+(\varphi; \mathbf{s}, t), & \text{otherwise.} \end{cases}$$

Notice that the value 0 does not strictly imply falsification here since it is possible that $\rho(\varphi; \mathbf{s}, t) = 0$. Observe that the effective range of φ depends also on the signal \mathbf{s} and time t not only on the ranges of the respective signals.

Suppose that \mathbf{s} and \mathbf{s}' are two signals and that $\bar{\rho}(\varphi; \mathbf{s}, t) \leq \bar{\rho}(\varphi; \mathbf{s}', t)$. Then it is not necessarily true that $\rho(\varphi; \mathbf{s}, t) \leq \rho(\varphi; \mathbf{s}', t)$, that is, the signal \mathbf{s} is not closer to falsifying φ than the signal \mathbf{s}' in the absolute sense. It is, however, closer to falsifying in the proportional sense.

Let $\pi_i(\mathbf{v})$ be the projection of a vector \mathbf{v} to its i th coordinate. We assume that, for all i , there exists two real-valued mappings $t \mapsto \mathcal{I}_i^-(t)$ and $t \mapsto \mathcal{I}_i^+(t)$ such that $\pi_i(\mathbf{s}(t)) \in [\mathcal{I}_i^-(t), \mathcal{I}_i^+(t)]$ for all $t \in \mathbb{T}$. In practice, we fix a range $[A_i, B_i]$ for the i th signal component, that is, we assume that the mappings \mathcal{I}_i^- and \mathcal{I}_i^+ are constant.

Our aim is to build mappings $\mathcal{I}^-, \mathcal{I}^+ : \mathbb{T} \rightarrow \mathbb{R}$ such that $\rho(\varphi; \mathbf{s}, t) \in [\mathcal{I}^-(\varphi; t), \mathcal{I}^+(\varphi; t)]$ for all $t \in \mathbb{T}$. We then define the effective range $\mathcal{I}(\varphi; \mathbf{s}, t)$ of an STL formula φ to be $[\mathcal{I}^-(\varphi; t), \mathcal{I}^+(\varphi; t)]$.

Let $\mathcal{I}^-, \mathcal{I}^+ : \mathbb{T} \rightarrow \mathbb{R}$ be functions such that $\rho(\varphi; \mathbf{s}, t) \in [\mathcal{I}^-(\varphi; t), \mathcal{I}^+(\varphi; t)]$ for all $t \in \mathbb{T}$. For our applications, we need to discuss how to define \mathcal{I}^- and \mathcal{I}^+ appropriately for simple inequalities $X \geq Y$. Here we simply set

$$\begin{aligned}\mathcal{I}^-(X \geq Y; \mathbf{s}, t) &= \mathcal{I}^-(X; \mathbf{s}, t) - \mathcal{I}^+(Y; \mathbf{s}, t) \quad \text{and} \\ \mathcal{I}^+(X \geq Y; \mathbf{s}, t) &= \mathcal{I}^+(X; \mathbf{s}, t) - \mathcal{I}^-(Y; \mathbf{s}, t).\end{aligned}$$

This obviously satisfies our requirements.

Let us then describe how to define \mathcal{I}^- and \mathcal{I}^+ for general STL formulas. It is natural to set

$$\begin{aligned}\mathcal{I}^-(\neg\varphi; \mathbf{s}, t) &= -\mathcal{I}^+(\varphi; \mathbf{s}, t) \quad \text{and} \\ \mathcal{I}^+(\neg\varphi; \mathbf{s}, t) &= -\mathcal{I}^-(\varphi; \mathbf{s}, t).\end{aligned}$$

It is clear that this achieves our aim for the negation $\neg\varphi$.

Let us then consider the until operator and the formula $\varphi \mathcal{U}_{\mathcal{I}} \psi$. Inspired by (4), let $h(t')$ be the least integer in $[t, t')$ such that

$$\rho(\varphi; \mathbf{s}, h(t')) = \min_{t'' \in [t, t')} \rho(\varphi; \mathbf{s}, t'').$$

Similarly $u(t)$ be the least integer in $t + \mathcal{I}$ such that

$$\rho(\varphi \mathcal{U}_{\mathcal{I}} \psi; \mathbf{s}, t) = \min \{ \rho(\psi; \mathbf{s}, u(t)), \rho(\varphi; \mathbf{s}, h(u(t))) \}.$$

If $\rho(\psi; \mathbf{s}, u(t)) \leq \rho(\varphi; \mathbf{s}, h(u(t)))$, then we set

$$\mathcal{I}^-(\varphi \mathcal{U}_{\mathcal{I}} \psi; \mathbf{s}, t) = \mathcal{I}^-(\psi; \mathbf{s}, u(t)) \quad \text{and} \quad \mathcal{I}^+(\varphi \mathcal{U}_{\mathcal{I}} \psi; \mathbf{s}, t) = \mathcal{I}^-(\varphi; \mathbf{s}, h(u(t)))$$

otherwise. $\mathcal{I}^+(\varphi \mathcal{U}_{\mathcal{I}} \psi; \mathbf{s}, t)$ is defined analogously by substituting \mathcal{I}^- for \mathcal{I}^+ . With the convention that the effective range for the true signal \top is $[\infty, \infty]$, we obtain that

$$\mathcal{I}^-(\diamond_{\mathcal{I}}\varphi; \mathbf{s}, t) = \mathcal{I}^-(\varphi; \mathbf{s}, v_{\diamond}(t)) \quad \text{and} \quad \mathcal{I}^+(\diamond_{\mathcal{I}}\varphi; \mathbf{s}, t) = \mathcal{I}^+(\varphi; \mathbf{s}, v_{\diamond}(t))$$

where $v_{\diamond}(t)$ is the least integer in $t + \mathcal{I}$ such that $\rho(\diamond_{\mathcal{I}}\varphi; \mathbf{s}, t) = \rho(\varphi; \mathbf{s}, v_{\diamond}(t))$. Analogously

$$\mathcal{I}^-(\square_{\mathcal{I}}\varphi; \mathbf{s}, t) = \mathcal{I}^-(\varphi; \mathbf{s}, v_{\square}(t)) \quad \text{and} \quad \mathcal{I}^+(\square_{\mathcal{I}}\varphi; \mathbf{s}, t) = \mathcal{I}^+(\varphi; \mathbf{s}, v_{\square}(t))$$

where $v_{\square}(t)$ is the least integer in $t + \mathcal{I}$ such that $\rho(\square_{\mathcal{I}}\varphi; \mathbf{s}, t) = \rho(\varphi; \mathbf{s}, v_{\square}(t))$.

Consider finally the conjunction $\varphi \wedge \psi$ of two formulas. Let ζ be the formula such that $\rho(\varphi \wedge \psi; \mathbf{s}, t) = \rho(\zeta; \mathbf{s}, t)$ (in the case of equal robustness, we make an arbitrary but deterministic choice). We define

$$\mathcal{I}^-(\varphi \wedge \psi; \mathbf{s}, t) = \mathcal{I}^-(\zeta; \mathbf{s}, t)$$

and similarly for \mathcal{I}^+ .

Having defined \mathcal{I}^- and \mathcal{I}^+ like above, it is clear that we have constructed the required mappings \mathcal{I}^- and \mathcal{I}^+ for an arbitrary STL formula φ .

4.2.2 An Example on Scaling

Let us take a look at the formula

$$\varphi := \square_{[0,10]}(\text{SPEED}(t) < 50) \vee \diamond_{[0,30]}(\text{RPM}(t) > 2700),$$

and suppose that $\text{SPEED}(t) \in [0, 120]$ and $\text{RPM}(t) \in [0, 4800]$ for all t . Let \mathbf{s} be the vector-valued signal $t \mapsto (\text{SPEED}(t), \text{RPM}(t))$. The range of $\rho(\text{SPEED}(t) < 50; \mathbf{s}, t)$ is $[-70, 50]$ and the range of $\rho(\text{RPM}(t) > 2700; \mathbf{s}, t)$ is $[-2700, 2100]$.

Consider the situation where $\max_{t \leq 10} \text{SPEED}(t) = 5$ and $\max_{t \leq 30} \text{RPM}(t) = 1000$. Clearly

$$\rho(\Box_{[0,10]}(\text{SPEED}(t) < 50); \mathbf{s}, 0) = 50 - \max_{t \leq 10} \text{SPEED}(t) = 45$$

and

$$\rho(\Diamond_{[0,30]}(\text{RPM}(t) > 2700); \mathbf{s}, 0) = \max_{t \leq 30} \text{RPM}(t) - 2700 = -1700.$$

Therefore $\rho(\varphi; \mathbf{s}, 0) = 45$. Now if we naively take the scaling range to be $[-2700, 2100]$, which is the smallest interval containing the ranges of the predicates, then we end up with a scaled robustness of $45/2100 \approx 0.02$. This seems to indicate that the input signal is close to falsifying the requirement φ , but this is obviously a wrong impression as the component $\text{SPEED}(t)$ is very far away from being a falsifying signal.

Let us compute the scaled robustness metric as defined in Subsection 4.2.1. The formula φ is a conjunction of two formulas, and thus the effective range for φ equals the effective range of the subformula whose robustness at time $t = 0$ evaluates to a larger value. Above we saw that this corresponds to the left subformula. Moreover, as the effective ranges of propositions are constant, it is irrelevant where the minimum corresponding to the always operator is attained. Consequently

$$\mathcal{I}(\varphi; \mathbf{s}, 0) = \mathcal{I}(\Box_{[0,10]}(\text{SPEED}(t) < 50); \mathbf{s}, 0) = \mathcal{I}(\text{SPEED}(t) < 50; \mathbf{s}, 0) = [-70, 50].$$

Therefore $\bar{\rho}(\varphi; \mathbf{s}, 0) = 45/50 = 0.9$. This number is much more reasonable and indicates correctly that the input signal is not close to falsifying φ .

This example indicates that our scaled robustness metric can overcome problems related to naive scaling, and we propose to use our method based on the effective range whenever scaling STL robustness values is required.

5 Research Questions and Evaluation Methodology

In this section, we describe the details of a practical implementation of OGAN (Algorithm 1). In order to evaluate this implementation, we propose several research questions that we answer by conducting computational experiments in which we compare OGAN against state-of-the-art requirement falsification algorithms on standard benchmarks. We also present a novel methodology to analyze the experimental results. The research questions are answered to in Section 6.

5.1 Research Questions

A requirement falsification algorithm obviously must be able to falsify a requirement (if it is falsifiable). We call this falsification capability *effectiveness*, and we measure it using falsification rate, which is defined in Subsection 5.2. Our first research question is thus the following:

RQ1. Is OGAN effective on common falsification benchmarks?

Two algorithms can achieve the same effectiveness, but one algorithm can use significantly more resources than another. We deem that lowering the number of SUT executions needed for a falsification amounts to increased *efficiency*. We ask:

RQ2. Is OGAN efficient on common falsification benchmarks?

We study efficiency using methods from survival analysis; cf. Subsection 5.2.

Recall that initially the OGAN algorithm uses a Monte-Carlo sampling method to obtain the initial training data for the discriminator. It is reasonable to ask how the choice of the sampling strategy affects OGAN’s effectiveness and efficiency.

RQ3. Does the choice of Monte-Carlo sampling strategy affect OGAN’s performance?

We address this question by comparing two sampling strategies: uniform random sampling and Latin hypercube sampling.

A falsification algorithm that is effective and efficient in the above senses can use a lot of computational resources, which might be undesirable. OGAN trains neural networks, and this is known to be computationally expensive. This naturally leads to the following question:

RQ4. What is the computational overhead of OGAN?

The discriminator is trained to learn the relation between SUT inputs and the robustness. The purpose of the discriminator is only to allow the generator to learn to produce tests with low robustness. It is not clear how accurate the discriminator needs to be for a successful falsification. If it is accurate, then the discriminator could be used as a surrogate model in other tasks beyond requirement falsification. Thus, we ask the following question:

RQ5. Does OGAN train accurate discriminators?

Our final research question concerns the use of the generator to augment the discriminator’s training data. It is not clear a priori whether it is a good idea to focus on low-robustness tests produced by the generator or if it is a better idea to use samples independent of it.

RQ6. Does augmenting the discriminator’s training data by sampling the generator improve OGAN’s effectiveness and efficiency?

We study this by comparing OGAN against a variant whose generator sampling is disabled.

5.2 Evaluation Methodology

Here we propose a methodology to evaluate OGAN and answer the proposed research questions. We aim to outline a general methodology for studying the effectiveness and efficiency of requirement falsification algorithms. A widely used guide for the evaluation of randomized algorithms is presented in the survey [2]. Here we go beyond these recommendations and use methods from survival analysis that are not discussed in the survey. To the best of our knowledge, this has not been done in the context of evaluating requirement falsification algorithms.

Consider a benchmark, that is, a SUT and a requirement φ . A requirement falsification algorithm is naturally evaluated on its capability of being able to falsify φ with a given execution budget. As most requirement falsification algorithms are stochastic, this capability is not determined well by a single run of the algorithm, so several independent replicas are required for the assessment. This leads to the concept of *falsification rate* (FR) which is the proportion of successful falsifications over, say, N replicas. We take FR to be our evaluation criterion for effectiveness, and we deem an algorithm \mathcal{A} to be more effective than algorithm \mathcal{A}' if \mathcal{A} has higher FR than \mathcal{A}' .

Recall our assumption that evaluating the SUT output is expensive. Thus among two equally effective algorithms, the one that uses fewer executions is better: it is more efficient. A simple statistic \bar{S} for efficiency is the mean of the number of executions required for a falsification. The statistic \bar{S} , however, only considers successful replicas, and a noneffective algorithm may achieve low \bar{S} . This means that the number \bar{S} should be always interpreted together with the FR.

In order to compare falsification algorithms better, we propose to base the comparison on methods of survival analysis [28]. Consider a falsification algorithm \mathcal{A} for the falsification of a requirement φ of some SUT. Let $E_{\mathcal{A}}$ be the number of executions needed to falsify φ using \mathcal{A} , and set $E_{\mathcal{A}} = B^+$ (censored observation) if a falsifying input was not found within a given execution budget B . Thus $E_{\mathcal{A}}$ is a random variable and it can be interpreted as the survival time of φ when \mathcal{A} is used for falsification. Intuitively, the algorithm \mathcal{A} has better performance than an algorithm \mathcal{A}' if the survival times observed from $E_{\mathcal{A}}$ tend to be lower than those observed from $E_{\mathcal{A}'}$.

A natural way to visualize survival times is to plot the survival function S defined by setting

$$S(t) = \mathbb{P}(E_{\mathcal{A}} > t).$$

This function can be estimated using the Kaplan–Meier estimator \hat{S} [28, Sec. 1.4] defined as

$$\hat{S}(t) = \prod_{1 \leq i \leq t} \left(1 - \frac{d_i}{n_i}\right)$$

where d_i is the number of patients that have died since time $i - 1$ (the number executions of \mathcal{A} that managed to falsify φ in exactly i executions) and n_i is the number of patients at risk (the number of executions of \mathcal{A} that have not been censored and have not been able to falsify φ with at most $i - 1$ executions). See Figure 5 for example survival functions (the light areas correspond to 95% confidence intervals; see below).

Here censoring happens only when the execution budget B is exhausted, and in this case it can be easily proved that the final value $\hat{S}(B)$ equals $1 - F$ where F is the falsification rate $\sum_{i=1}^B d_i/N$. This connection is convenient as it allows us to compute confidence intervals for the FR. See [6, Sec. 1.4] for more on confidence intervals for $\hat{S}(t)$ based on the $\log(-\log(\cdot))$ transformation.

Estimating the survival function thus serves two purposes. First, it yields the FR and a confidence interval for it. Second, the survival function can be used for a further comparison of algorithms achieving similar FR values. Indeed, if the survival function for an algorithm \mathcal{A} decreases faster than that of an algorithm \mathcal{A}' , then \mathcal{A} tends to falsify the requirement with fewer SUT executions than \mathcal{A}' . From this observation, it follows that we should test if the distributions of $E_{\mathcal{A}}$ and $E_{\mathcal{A}'}$ are the same. Under the hypothesis that the distributions are identical, the log-rank statistic [28, Sec. 1.5] is asymptotically χ_1^2 -distributed and can be used for computing p -values. In this paper, we test the hypothesis of identical distributions, but we do not provide an explicit alternative hypothesis. This would require modeling the random variables $E_{\mathcal{A}}$ and $E_{\mathcal{A}'}$, and we have not attempted to do so. Without an explicit alternative, we do the analysis on case-by-case basis. For example, the p -value in Table 6 supports that the survival functions of OGAN US and OGAN LHS are not identical in the AT1₂₀ benchmark. From Figure 3, it is evident that, even though the FRs are similar, OGAN US tends to require fewer executions than OGAN LHS.

In addition, the survival function can be used to give a baseline assessment on how difficult a given benchmark is. We propose to do this as follows: use uniform random search as the falsification algorithm on two benchmarks and compare the estimated survival functions. The benchmark for which the survival function reaches the lowest value the fastest can be deemed to be the easier benchmark. For example, based on Figure 3, we consider the benchmark AT6_{30,80,4500} to be easier than AT6_{30,50,2700}.

We remark that typical assumptions in survival analysis such as proportional hazards [28, Ch. 4] do not seem to apply (see Figures 3, 4). Notice also that we have decided not to model in the effect of the initial random sampling that is present in OGAN.

Summarizing the above, we evaluate a falsification algorithm as follows: on each benchmark, we report the falsification rate FR and its 95% confidence interval (CI). We display the estimated survival functions in order to compare the performances of several algorithms on a given benchmark. In addition, we report the mean number \bar{S} of executions required for a falsification.

5.3 Benchmark Selection

For our evaluation, we mainly use the benchmarks of the ARCH-COMP 2023 competition [33]. In addition, we include some benchmarks from [15]. These problems represent a varied selection of systems, and they have been used for the evaluation of requirement falsification algorithms on numerous occasions [13, 14, 33, 15].

For brevity, we have excluded from this report benchmarks that we deem as too easy. Our exclusion criterion is as follows: we do not report results for a benchmark if uniform random search can achieve a falsification rate greater than 0.5 with a budget of 75 executions over 50 repetitions. This criterion excludes the benchmarks AFC29, AT2, AT51, AT52, AT53, AT54, CC1, CC2, and CC5 from [33]. We also exclude benchmarks of [33] that at most one algorithm could falsify as there is no comparison to be made. This criterion excludes the benchmarks SC and AFC33. We remark that OGAN is not able to falsify the requirements of these two difficult

benchmarks. Finally, we exclude the benchmarks AT6ABC, CCX, NNX, and AT6ABC because they concern the falsification of multiple requirements, and we only focus on the falsification of a single requirement in this paper.

Next we list the benchmarks used in our experiments. In each benchmark, we have used a sampling rate of 0.01 for discretizing the input and output signals.

Automotive Powertrain Fuel Control (AFC). This benchmark is proposed in [27]. Given two input signals θ (throttle) and ω (brake), the model outputs a signal μ (normalized deviation from a reference value). As in the ARCH-COMP 2023 competition, we assume that

$$\theta(t) \in [0, 61.2], \quad \omega(t) \in [900, 1100], \quad \text{and} \quad \mu(t) \in [-1, 1]$$

for all t during the simulation time of 50 time units. The input signals are piecewise constant signals. The throttle θ consists of 10 segments of 5 time units and the brake ω is constant. We use the following requirement:

$$\text{AFC27} = \square_{t \in [11, 50]} ((\text{rise}(t) \vee \text{fall}(t)) \rightarrow (\square_{t' \in [1, 5]} |\mu(t')| < \beta)) \text{ and}$$

where $\beta = 0.008$ and

$$\begin{aligned} \text{rise}(t) &= (\theta(t) < 8.8) \wedge (\diamond_{t' \in [0, 0.05]} \theta(t') > 40.0) \text{ and} \\ \text{fall}(t) &= (\theta(t) > 40.0) \wedge (\diamond_{t' \in [0, 0.05]} \theta(t') < 8.8). \end{aligned}$$

The requirement expresses that after the throttle has risen or fallen, the deviation from the reference value should decrease soon and stay low for a while.

Automatic Transmission (AT). This model is from Mathworks and has been proposed as a benchmark in [25]. Given two input signals THROTTLE and BRAKE, the model outputs three signals: v (speed of the modeled car), ω (engine speed of the car in RPM), and g (currently selected gear). As in the ARCH-COMP 2023 competition, we assume that

$$\text{THROTTLE}(t) \in [0, 100] \quad \text{and} \quad \text{BRAKE}(t) \in [0, 325]$$

for all t during the simulation time of 30 time units. We assume that the input signals are piecewise constant signals consisting of 6 segments of 5 time units in accordance with [33]. For the output signals, we set the following ranges:

$$v(t) \in [0, 125], \quad \omega(t) \in [0, 4800], \quad \text{and} \quad g(t) \in \{1, 2, 3, 4\}$$

for all t .

In our experiments, we consider the requirements (with obvious interpretations) from [33, 15] defined by the following templates:

$$\begin{aligned} \text{AT1}_T &= \square_{t \in [0, T]} v(t) < 120, \\ \text{AT6}_{T, v, \omega} &= (\square_{t \in [0, 30]} \omega(t) < \omega) \rightarrow (\square_{t \in [0, T]} v(t) < v), \text{ and} \\ \text{ATX2} &= \neg(\square_{t \in [10, 30]} v(t) \in [50, 60]). \end{aligned}$$

Chasing Cars (CC). This model is derived from [26]. This is another car model which takes inputs THROTTLE and BRAKE, and outputs the location Y_1 of a car and locations Y_2, Y_3, Y_4, Y_5 of cars chasing it. We assume that

$$\text{THROTTLE}(t), \text{BRAKE}(t) \in [0, 1]$$

for all t during the simulation of 100 time units. The input signals are piecewise constant signals consisting of 20 segments of 5 time units as in [33]. Experimentally we have decided to use

respectively the ranges $[-250, 0]$, $[-240, 10]$, $[-230, 20]$, $[-220, 30]$, and $[-210, 40]$ for the signals Y_1, \dots, Y_5 . The following requirements are found in [33]:

$$\begin{aligned} \text{CC3} &= \square_{t \in [0, 80]} ((\square_{t' \in [0, 20]} Y_2(t') - Y_1(t') \leq 20) \vee (\diamond_{t' \in [0, 20]} Y_5(t) - Y_4(t) \geq 40)), \text{ and} \\ \text{CC4} &= \square_{t \in [0, 65]} \diamond_{t' \in [0, 30]} \square_{t'' \in [0, 20]} Y_5(t'') - Y_4(t'') \geq 8. \end{aligned}$$

F-16 Ground Collision Avoidance (F16). A version of this model has been presented in [24]. The model controls an aircraft and attempts to avoid ground collisions. The input for the model is a vector (not a signal) with three components ROLL, PITCH, and YAW which determine the orientation of the aircraft in the starting position at the altitude of 4040 feet. As in [33], we set

$$\text{ROLL} \in [0.2\pi, 0.2833\pi], \text{ PITCH} \in [-0.4\pi, -0.35\pi], \text{ and } \text{YAW} \in [-0.375\pi, -0.125\pi].$$

The output of the model is a signal ALTITUDE representing the altitude of the aircraft during the simulation of 15 time units. The only requirement is the following:

$$\text{F16} = \square_{t \in [0, 15]} \text{ALTITUDE}(t) > 0.$$

In our experiments, we use the range $[0, 4040]$ for the output signal.

We stress that there are many versions of the F16 model; see for example the Python implementation². We have observed different models can have wildly different behavior especially if the input ranges are modified. We use the Matlab implementation and signal ranges presented in [33].

Observe that a requirement falsification algorithm that requires nonatomic testing cannot be used to falsify the requirement F16 because the input is not a signal.

Neural Network Controller (NN). This model is a neural network controller for magnet levitation at a reference position based on an example from Mathworks³. The input signal is a reference position R and the output P is the current position of the magnet. We use the following requirement template from [33]:

$$\begin{aligned} \text{NN}_\beta &= \square_{t \in [1, 37]} (|P(t) - R(t)| > \alpha + \beta |R(t)| \\ &\rightarrow \diamond_{t' \in [0, 2]} \square_{t'' \in [0, 1]} |P(t'') - R(t'')| < \alpha + \beta |R(t'')|) \end{aligned}$$

where $\alpha = 0.005$. The simulation time is 40 time units, and we assume that the input signal consists of 3 segments of 40/3 time units. For the requirement NN_β , we assume that $R(t) \in [1, 3]$ for all t , and we assume that $R(t) \in [1.95, 2.05]$ for all t in the case of the other requirement. For the output position P , we use the range $[0, 4]$.

Pacemaker (PM). This model is a simple controller of a pacemaker device described in [3]. The output is the PACECOUNT signal which counts how many heart paces have been observed since the beginning of the simulation (this is a nondecreasing discrete-valued signal). The input is the lower rate limit signal LRL. It specifies the minimum amount of paces per minute that the pacemaker should achieve. We assume that $\text{LRL}(t) \in [50, 90]$ for all t and that LRL is piecewise constant signal consisting of 5 segments of 2 time units for a total a total length of 10 time units. The input signal values can be arbitrary floating point numbers in the interval $[50, 90]$, but they are rounded to the nearest integer internally. We consider the following requirement given in [3]:

$$\text{PM} = \square_{t \in [0, 10]} \text{PACECOUNT}(t) \leq 15 \wedge \diamond_{t \in [0, 10]} \text{PACECOUNT}(t) \geq 8.$$

It specifies that the observed pacing should match the requested LRL. Indeed, 90 paces in a minute correspond to 15 paces in 10 seconds and 50 paces a minute to 8 paces in 10 seconds.

²<https://github.com/stanleybak/AeroBenchVVPython>

³<https://www.mathworks.com/help/deeplearning/ug/design-narma-12-neural-controller-in-simulink.html>

5.4 OGAN Setup for Experiments

This section describes what choices we have made in setting up Algorithm 1 for the experiments. We have refrained from tuning the parameters for each benchmark separately, and we describe a common setup that has good overall performance. Our description is a distillation of our experience with OGAN so far and can be taken as a good initial setup in subsequent experiments.

Representation of System Inputs. As described in Subsection 5.3, with the exception of the benchmark F16, the inputs of the benchmarks are piecewise constant signals of equal piece length. Such a one-dimensional signal consisting of D pieces that takes values in the interval $[A, B]$, $A < B$, can be described fully by D numbers. We map these numbers to the interval $[-1, 1]$ using the linear map $x \mapsto (-2x + A + B)/(A - B)$. We thus take the input space to be $[-1, 1]^D$ and map its vectors to SUT inputs using the inverse transformation. If the benchmark input is a vector, not a signal, then we do the same but omit the sampling of the inverse images into a signal. In the case of a multidimensional signal, we simply concatenate the vector representations of its one-dimensional components into a single long vector.

We have assumed here that the signal ranges (which can be different between components) are known in advance. Some ranges must be specified as OGAN cannot be used otherwise.

Scaled Robustness Metric. OGAN uses an implementation of the scaled robustness metric defined in Subsection 4.2.1.

Dimension of the Latent Space. In the experiments, the dimension of the input space (see Subsection 2.4 and Subsection 5.3) takes values in $\{3, 11, 12, 40\}$. Intuitively it is easier to learn a mapping from a higher-dimensional space to a lower-dimensional space, so we have made the decision to set the latent space dimension D to be 20. This is smaller than the input space dimension for the CC benchmark, but this does not seem to matter.

Discriminator and Generator Models. Since our execution budgets are low (300, 1500), the training data is rather small. Thus it would be unreasonable to use large or deep neural network models. In all cases, the generator network is a fully connected network with three hidden layers of 128 neurons. We use tanh activation for the output (since the tests components are elements of $[-1, 1]$) and leaky ReLU with negative slope 0.01 for other activations.

In all experiments with input signals, that is, all excluding F16, we use a convolutional network for the discriminator. We use two convolutional layers of 16 feature maps with kernel size 2, stride 1, and 0-padding 1 followed by a leaky ReLU activation with negative slope 0.01 and a maxpool layer with window size 2 and stride 2. The convolutional layer is flattened and mapped to a hidden layer of 128 neurons (no activation). The output of this final layer is fed through the sigmoid function to produce a single number. The input in the F16 benchmark cannot be understood as a signal or a time series, and we use the above generator setup with sigmoid output activation.

We have observed that the proposed models have large enough capacity to overfit to a training data of 300 samples (with the number of epochs described below).

In both the generator and the discriminator, we initialize the weights using the Glorot-Bengio initialization [20] with layers that use a tanh or sigmoid activation and the He et al. initialization [23] for layers with ReLU activations.

Training of the Neural Networks. We use a modified squared error as the loss function used in training of both \mathcal{D} and \mathcal{G} . Since our robustness metric takes values in $[0, 1]$, the squared error does not penalize for errors in a correct way. Instead, we propose the following. Let $F(x) = \text{logit}(0.98x + 0.01)$ where $\text{logit}(x) = \log x/(1 - x)$ (the constants 0.98 and 0.01 are arbitrary, and their purpose is to avoid singularities when $x = 0$ or $x = 1$). We let

$$\mathcal{L}(\hat{y}, y) = (F(\hat{y}) - F(y))^2 + \lambda \left(F\left(\frac{1}{2} - \frac{\hat{y} - y}{2}\right) - F\left(\frac{1}{2}\right) \right)^2$$

with $\lambda = 0.001$. The first summand of the loss function encourages the network to minimize errors especially when the ground truth is close to 0 or 1. This is exactly what we need: the discriminator does not need to be perfect, it just needs to predict “large” when the ground truth is “large” and “small” when the ground truth is “small”. The second summand softly enforces our wish that $y = \hat{y}$. Indeed, the function F is symmetric about $1/2$ so, in principle, the first term could be minimized by setting $y \approx 1$ when $\hat{y} \approx 0$ (or vice versa). We have not observed this behavior in our experiments, but it is better to be safe than sorry.

We use the Adam optimizer for training both \mathcal{D} and \mathcal{G} . We use the default values 0.9 and 0.999 for the beta parameters and learning rates 0.005 and 0.0001 for the discriminator and the generator respectively. We used the hyperparameter tuning and found that this combination of learning rates gave the best overall performance on all benchmarks when the learning rates were selected from the set $\{0.5, 0.1, 0.05, 0.01, 0.005, 0.001, 0.0005, 0.0001\}$. We recommend to start with the selected learning rates in any subsequent study. Based on our experience, we suggest that the discriminator learning rate should be larger than the generator learning rate.

We use 15 training epochs for the discriminator and, on each epoch, we train on a single batch consisting of the complete training data so far. We have not considered any mechanisms to prevent harmful overfitting but, based on our experience with the benchmarks, it seems that this setup is good enough so that the discriminator can generalize and generators trained on it can accomplish their task. With the generator, we use 375 epochs with batch size 32 (i.e., $B = 32$ in Algorithm 1). This overfits the generator on the discriminator to some degree which means that the generator will produce tests that are quite similar to each other. As long as the discriminator is of good quality, this has no practical implications when the objective is to find one single falsifying input as is the case in these benchmarks.

Other. We set $\alpha = 0.95$ (see the line 24 of Algorithm 1).

5.5 Baseline and Data Collection

We compare OGAN to a uniform random search algorithm and a total of eleven tools that participated in the ARCH-COMP 2021 and 2023 competitions [13, 33]. For brief introductions to these tools, see Section 7. The experiment results were collected on a desktop PC running Ubuntu 22.04 with an Intel i9-10900X CPU, a NVIDIA GeForce RTX 3090 GPU, and 64 GB of RAM. The results necessary for recreating the tables and figures of this article are available at <https://dx.doi.org/10.5281/zenodo.8382845>.

5.6 Replication of Experiment Results

OGAN is implemented as a part of the STGEM falsification framework, which was used to obtain the results presented in this paper. STGEM can perform different testing tasks, including requirement falsification, when provided with a suitable executable function for the SUT and the requirements. STGEM supports several search algorithms such as OGAN, WOGAN [38], grid search, random sampling algorithms, and several evolutionary algorithms. It can also combine different algorithms such as a random sampling algorithm and OGAN in the same falsification task. This is how the initial training data is collected for OGAN. The different search algorithms are independent of each other and can be applied sequentially or in parallel.

STGEM can tune the hyperparameters of its algorithms. In fact, any of its algorithms can be used for the hyperparameter search. It also has facilities for executing computational experiments and running multiple replicas of a falsification task. Careful use of the random number generator ensures that the results are replicable. STGEM is written in Python and uses high performance libraries, such as Numpy and PyTorch, for mathematical operations and machine learning.

A SUT in STGEM can be defined as a Python class, as a Matlab Simulink model, or as an external operating system process. STGEM has full support for requirements in STL including an implementation of the scaled robustness metric of Subsection 4.2.1). It is also possible to define a custom requirement monitor and robustness metric.

The STGEM framework and its implementation of the OGAN algorithm is freely available at <https://gitlab.abo.fi/stc/stgem>. The benchmarks presented in this paper are available at <https://gitlab.abo.fi/stc/experiments/ogan> along with the repeatability instructions.

6 Experiment Results

6.1 RQ1 and RQ2: Effectiveness and Efficiency

Recall that the effectiveness of a requirement falsification algorithm measures its capability of being able to falsify a requirement. RQ1 asks if OGAN is effective on common falsification benchmarks. RQ2 asks the same for efficiency; increased efficiency means fewer needed SUT executions. We answer RQ1 and RQ2 by comparing OGAN’s effectiveness and efficiency to those of the requirement falsification algorithms from the ARCH-COMP 2021 and 2023 competitions and [15]. We omit ARCH-COMP 2022 results since including them would add very little to the below comparisons.

6.1.1 Comparison to ARCH-COMP 2023 Tools

Table 1 and Figures 1 and 2 report the results of the ARCH-COMP 2023 competition [33] for the benchmarks of Subsection 5.3. The reported data is based on the results collected by the competition organizers⁴. The competition report only states the statistics FR and \bar{S} . We estimated the confidence intervals and survival functions from the data using the methods described in Subsection 5.2. The results are based on only 10 replicas and the reported confidence intervals are quite wide due to the small sample size. For completeness sake, we include the results for the benchmarks ATX2, AT6_{30,80,4500}, and AT6_{30,50,2700} which were not part of the competition.

The algorithms of ARCH-COMP 2023 are described in more detail in Section 7. Table 2 indicates which tools use atomic test execution and which of them use precollected data or models. Recall that OGAN uses atomic test execution and does not use any previous data or models.

The ARCH-COMP 2023 used an execution budget of 1500 tests. The input parametrization was the same as described in Subsection 5.4. OGAN was configured as described in Subsection 5.4. The initial Monte Carlo sampling was chosen to be uniform random sampling with an execution budget of 75. The sampling probability was set to 0.21 which means that, on average, 375 (25% of 1500) uniform random samples were executed during the total budget of 1500 executions.

From the results, we see that, with the exception of the benchmarks CC4, F16, and NN_{0,04}, OGAN has full FR and the survival function decay is among the fastest. The benchmark CC4 appears impossible for OGAN to falsify. This appears to be the case for all algorithms except FORESEE. Data for the F16 benchmark is reported by only two algorithms: ATheNA and OGAN. ATheNA clearly wins OGAN in effectiveness and efficiency. We remark that ATheNA uses hand-crafted robustness metrics for each benchmark [18]. This can be seen as use of precollected information, and it is unclear how it affects ATheNA’s performance. Finally, in the NN_{0,04} benchmark OGAN achieves the best FR. The sample size is small, so we cannot confidently say that OGAN is better than ARISTEO on this benchmark.

6.1.2 Comparison to ARCH-COMP 2021 Tools

Tables 3 and 4 report the results of the ARCH-COMP 2021 competition [13] and the article [15] together with the corresponding results for the OGAN algorithm. Both sources have a common execution budget of 300 executions. Unfortunately no data is available to compute confidence intervals or survival functions, so we merely report the statistics FR and \bar{S} . The input parametrization is the same as in Subsection 5.3. The reported results are based on 50 independent replicas, so the results are more reliable than those reported above.

The OGAN setup is as in Subsection 5.4. We use 75 initial random samples obtained via uniform random sampling. The sampling probability P is set to 0.

⁴<https://dx.doi.org/10.5281/zenodo.8024426>

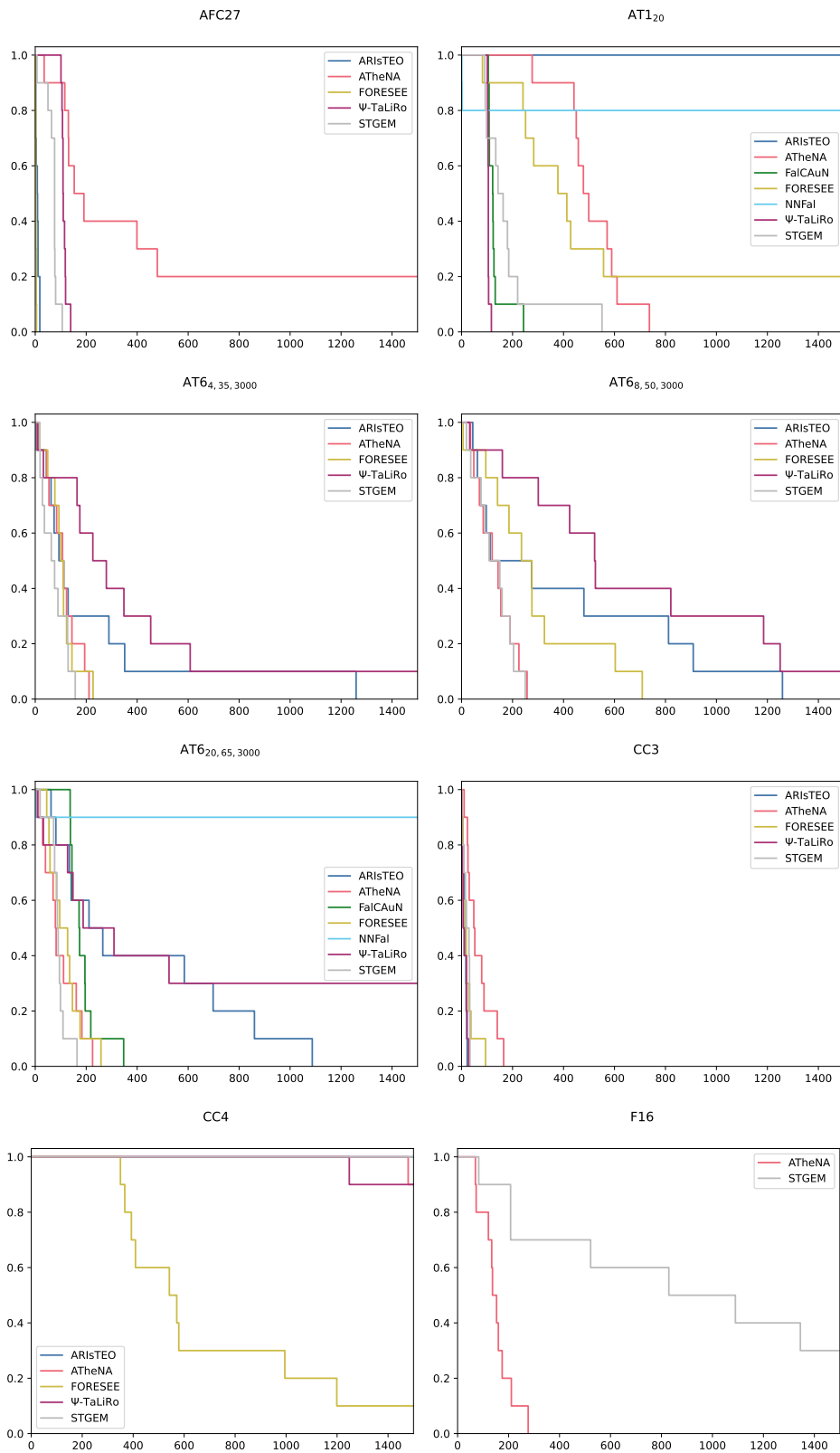


Figure 1: Survival functions for ARCH-COMP 2023 tools on benchmarks from Subsection 5.3. The light areas correspond to 95% confidence intervals.

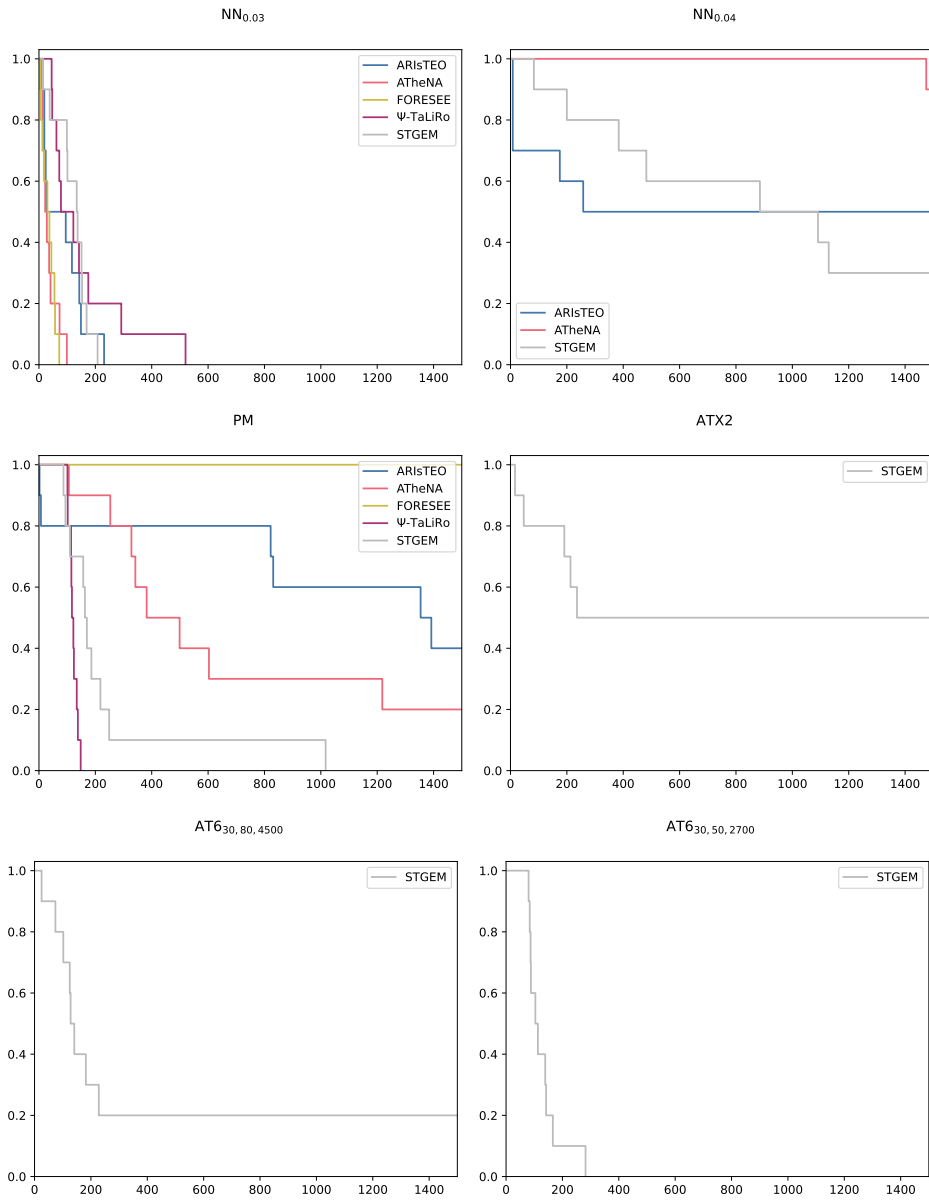


Figure 2: Figure 1 continued.

Req.	ARIsTEO: ARX-2			ATheNA:			FalCAuN:			FORESEE:			NNFal:			Ψ -TaLiRo: ConBo			STGEM: OGAIN		
	FR	95% CI	\bar{S}	FR	95% CI	\bar{S}	FR	95% CI	\bar{S}	FR	95% CI	\bar{S}	FR	95% CI	\bar{S}	FR	95% CI	\bar{S}	FR	95% CI	\bar{S}
AFC27	1.00	[1.00, 1.00]	8.5	0.80	[0.53, 0.97]	204.2	1.00	[1.00, 1.00]	2.6	1.00	[1.00, 1.00]	2.6	1.00	[1.00, 1.00]	113.2	1.00	[1.00, 1.00]	113.2	1.00	[1.00, 1.00]	69.4
AT1 ₂₀	0.00	[0.00, 0.00]	–	1.00	[1.00, 1.00]	511.0	0.80	[0.53, 0.97]	329.1	0.20	[0.05, 0.59]	1.5	1.00	[1.00, 1.00]	105.4	1.00	[1.00, 1.00]	105.4	1.00	[1.00, 1.00]	185.8
AT6 _{4,35,3000}	1.00	[1.00, 1.00]	241.7	1.00	[1.00, 1.00]	108.1	1.00	[1.00, 1.00]	104.8	1.00	[1.00, 1.00]	104.8	0.90	[0.64, 0.99]	255.0	0.90	[0.64, 0.99]	255.0	1.00	[1.00, 1.00]	74.2
AT6 _{8,50,3000}	1.00	[1.00, 1.00]	412.4	1.00	[1.00, 1.00]	132.7	1.00	[1.00, 1.00]	285.2	1.00	[1.00, 1.00]	285.2	0.90	[0.64, 0.99]	580.0	0.90	[0.64, 0.99]	580.0	1.00	[1.00, 1.00]	128.3
AT6 _{20,65,3000}	1.00	[1.00, 1.00]	412.4	1.00	[1.00, 1.00]	132.7	1.00	[1.00, 1.00]	117.8	0.10	[0.01, 0.53]	3.0	1.00	[1.00, 1.00]	191.1	0.70	[0.42, 0.93]	191.1	1.00	[1.00, 1.00]	89.6
CC3	1.00	[1.00, 1.00]	12.8	1.00	[1.00, 1.00]	66.0	1.00	[1.00, 1.00]	22.4	1.00	[1.00, 1.00]	22.4	1.00	[1.00, 1.00]	11.7	1.00	[1.00, 1.00]	11.7	1.00	[1.00, 1.00]	20.3
CC4	0.00	[0.00, 0.00]	–	0.10	[0.01, 0.53]	1479.0	0.90	[0.64, 0.99]	600.6	0.10	[0.01, 0.53]	–	0.90	[0.64, 0.99]	1248.0	0.10	[0.01, 0.53]	1248.0	0.00	[0.00, 0.00]	–
F16	–	–	–	1.00	[1.00, 1.00]	151.1	–	–	–	–	–	–	–	–	–	0.70	[0.42, 0.93]	612.1	0.70	[0.42, 0.93]	612.1
NN _{0.03}	1.00	[1.00, 1.00]	83.7	1.00	[1.00, 1.00]	35.8	1.00	[1.00, 1.00]	33.6	–	–	–	1.00	[1.00, 1.00]	155.5	1.00	[1.00, 1.00]	155.5	1.00	[1.00, 1.00]	120.4
NN _{0.04}	0.50	[0.25, 0.82]	91.4	0.10	[0.01, 0.53]	1475.0	0.10	[0.01, 0.53]	–	–	–	–	0.10	[0.01, 0.53]	–	0.70	[0.42, 0.93]	607.7	0.70	[0.42, 0.93]	607.7
PM	0.60	[0.33, 0.88]	734.7	0.80	[0.53, 0.97]	466.4	0.00	[0.00, 0.00]	–	–	–	–	0.00	[0.00, 0.00]	–	1.00	[1.00, 1.00]	121.5	1.00	[1.00, 1.00]	166.5

Table 1: Falsification results over 10 independent replicas for ARCH-COMP 2023 tools. We report falsification rate (FR), i.e., the ratio of successful falsifications out of 10 trials, its 95% confidence interval, and mean number \bar{S} of executions required for a falsification.

	ARIsTEO		ATheNA		Breach		FalCAuN		falsify		FALSTAR		FORESEE		NNFal		Ψ -TaLiRo		S-TaLiRo		STGEM		zlscheck	
	✓	✗	✓	✗	✓	✗	✓	✗	✓	✗	✓	✗	✓	✗	✓	✗	✓	✗	✓	✗	✓	✗	✓	✗
Atomic test execution	✓		✓		✓		✓		✗	✗	✗	✗	✓	✓	✓	✓	✓	✓	✓	✓	✓	✓	✓	✗
No precollected data	✓		✗		✓		✓		✗	✗	✗	✓	✓	✓	✗	✗	✓	✓	✓	✓	✓	✓	✓	✗

Table 2: Information on which of the considered falsification algorithms use atomic testing and which use previously collected data or models.

Req.	ARIsTEO: ARX-2		Breach: GNM		FalCAuN:		falsify: A3C		FALSTAR: aLVTS		FORESEE:		S-TaLiRo: SOAR		STGEM: OGAN		zlscheck: GD	
	FR	\bar{S}	FR	\bar{S}	FR	\bar{S}	FR	\bar{S}	FR	\bar{S}	FR	\bar{S}	FR	\bar{S}	FR	\bar{S}	FR	\bar{S}
AFC27	1.00	2.3	1.00	3.0			1.00	1.6	1.00	3.9	1.00	2.8	1.00	70.3	1.00	76.8	1.00	1.0
AT1 ₂₀	0.00	–	0.00	–	0.92	171.2	0.78	125.8	1.00	33.0	0.58	252.3	1.00	170.3	0.82	119.1	1.00	2.3
AT6 _{4,35,3000}	0.94	103.1	0.00	–					1.00	76.1	0.98	117.0	0.88	130.4	1.00	88.0	1.00	42.7
AT6 _{8,50,3000}	0.90	164.7	0.00	–					1.00	82.4	0.78	180.2	0.78	207.2	1.00	132.4	0.10	129.5
AT6 _{20,65,3000}	0.98	89.1	0.00	–	1.00	214.1			0.00	–	0.94	124.6	0.84	197.5	0.96	92.3	0.04	261.7
CC3	1.00	18.9	1.00	28.6			0.88	13.5	0.08	207.5	1.00	14.4	1.00	22.4	1.00	23.7	1.00	23.4
CC4	0.00	–	0.00	–			0.18	120.4	0.00	–	0.26	311.1	0.00	–	0.00	–	0.64	124.6
F16	0.00	–	0.02	297.0									0.14	127.6	0.36	183.3	0.00	–
NN _{0,03}	1.00	62.8	1.00	6.0			1.00	1.00	0.52	177.0	1.00	44.2	0.98	68.0	0.98	76.0	1.00	1.3
NN _{0,04}													0.08	193.0	0.24	168.5	1.00	1.1

Table 3: Data is from [13, Tables 2,3] except for OGAN. Blanks indicate that data was not available. For the performance of uniform random search, see Table 5.

Req.	Breach: CMA-ES		FALSTAR: aLVTS		STGEM: OGAN	
	FR	\bar{S}	FR	\bar{S}	FR	\bar{S}
ATX2	1.00	145.2	1.00	86.3	0.48	159.2
AT6 _{30,80,4500}	1.00	97.0	1.00	22.8	0.88	103.8
AT6 _{30,50,2700}	0.98	46.7	1.00	47.6	0.92	120.2

Table 4: Data is from [15, Table 2] except for OGAN.

The results show that OGAN achieves full or almost full FR on all benchmarks except ATX2, CC4, F16, and NN_{0,04}. CC4 is again very hard for most algorithms to falsify. On the ATX2 benchmark, OGAN loses clearly to Breach and FALSTAR. Even though OGAN can achieve a higher FR with a bigger budget, as is evident from Figure 2, it appears to need at least an execution budget of 300 to achieve a FR at least 0.5; the algorithms Breach and FALSTAR are much more efficient. On the F16 benchmark OGAN achieves the best FR. On the NN_{0,04} benchmark, OGAN is the second best, but we remark that the astonishing performance of zlscheck is likely due to its ability of being able to access the internals of the SUT [13].

Comparing algorithm efficiency is now much harder in the absence of survival function estimates. The algorithm achieving the lowest \bar{S} varies from benchmark to benchmark. It is however safe to say that on all benchmarks OGAN does not have a markedly higher \bar{S} than the other algorithms. The only exception to this is perhaps the AFC27 benchmark where all algorithms except OGAN and S-TaLiRo achieve a very low \bar{S} . Nevertheless, we interpret the data to indicate that OGAN has efficiency that is comparable to the other algorithms.

Notice that if the OGAN survival functions of Figures 1 and 2 are truncated to 300 executions, the resulting FRs match quite closely those reported in Tables 3 and 4. This means that the two sampling strategies considered here (75 initial random samples, $P = 0.21$ and 75 random samples, $P = 0$) yield equivalent behavior up to 300 executions. Therefore increasing the execution budget and increasing exploration by raising P did not hamper OGAN’s ability to falsify with fewer executions than is in the budget.

6.1.3 The Answer

In the preceding two subsections, we argued that OGAN’s effectiveness and efficiency is comparable to the best-performing algorithms of ARCH-COMP 2021, [15], and ARCH-COMP 2023 on the majority of the considered benchmarks. OGAN is not uniformly best, but neither is any other algorithm. Since the goal of the ARCH-COMP competition is to compare state-of-the-art tools

for requirement falsification, we answer RQ1 and RQ2 as follows.

Answer to RQ1 and RQ2. OGAN has state-of-the-art requirement falsification efficiency and effectiveness.

It should also be noted that OGAN is the most general algorithm among the algorithms considered in this article. It supports benchmarks with signal inputs and benchmarks with vector inputs and does not use any precollected data or models.

6.2 RQ3: The Effect of the Chosen Monte-Carlo Sampling

In this subsection, we consider RQ3 which asks how the choice of the Monte-Carlo sampling strategy affects OGAN’s performance. We answer the question by considering two OGAN variants: OGAN US which uses uniform random sampling and OGAN LHS which uses Latin hypercube sampling (LHS). We also report how well pure uniform random search fares on the benchmarks. This provides information on how difficult the benchmarks are.

We use an execution budget of 300 (used in [13, 15]) and an initial random sampling budget $N = 75$ (25% of 300). We set the sampling probability P to 0 which means that we study how the initial random sampling strategy affects OGAN. Other settings are as in Subsection 5.4. Notice that the setup for OGAN US is the same as in Subsection 6.1.2, so the results for OGAN from that section match those of OGAN US. We ran 50 independent replicas of each falsification task. We used the same random seeds for the uniform random search and OGAN US, which means that the first 75 executions are identical for both algorithms.

Table 5 and Figures 3, 4 report the statistics chosen in Section 5 (the survival function for the benchmark CC4 is omitted as there is nothing to display). Table 6 reports the p -values of the logrank test under the null hypothesis that the survival functions of the two OGAN variants represent the same distribution. The column with heading RANDOM reports how uniform random search performs and thus establishes the baseline difficulty of the benchmarks.

Req.	p -value	US: LHS:	
		p -value	p -value
AFC27	0.428	0.98	0.93
AT1 ₂₀	0.014	0.79	0.02
ATX2	0.337	0.00	0.00
AT6 _{4,35,3000}	0.208	0.39	0.03
AT6 _{8,50,3000}	0.822	0.54	0.84
AT6 _{20,65,3000}	0.814	0.85	0.70
AT6 _{30,80,4500}	0.848	0.00	0.01
AT6 _{30,50,2700}	0.889	0.22	0.30
CC3	0.218	0.92	0.65
CC4	1.000	1.00	1.00
F16	0.217	0.08	0.19
NN _{0.03}	0.209	0.99	0.05
NN _{0.04}	0.605	0.95	0.15
PM	0.157	0.04	0.72

Table 6: Log-rank test p -values under the hypothesis that the survival functions of OGAN US and OGAN LHS represent the same distribution.

Table 7: Log-rank test p -values under the hypothesis that the survival functions of adaptive OGAN and nonadaptive OGAN represent the same distribution.

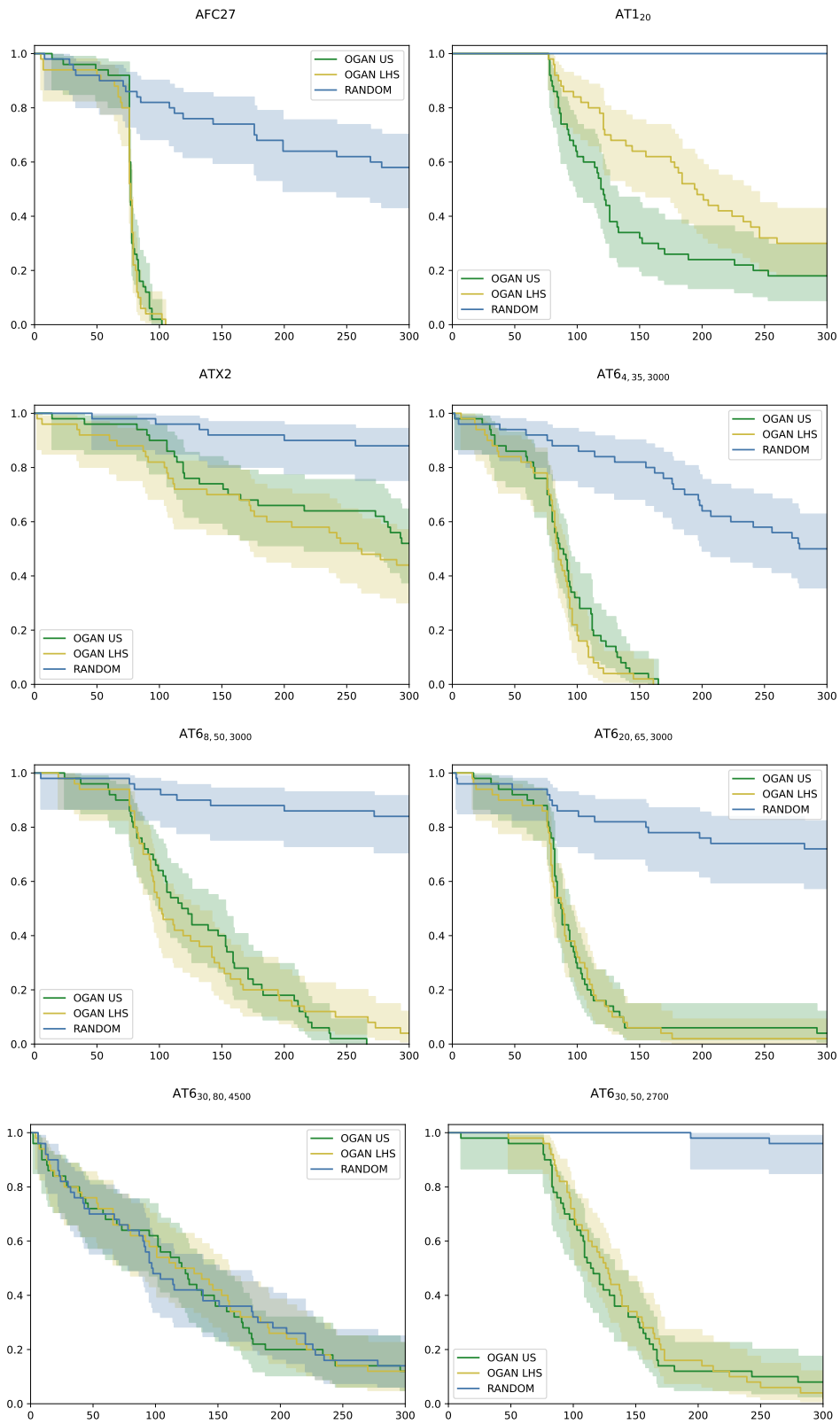


Figure 3: Survival functions for Random, OGAN US, and OGAN LHS for the benchmarks of Subsection 5.3

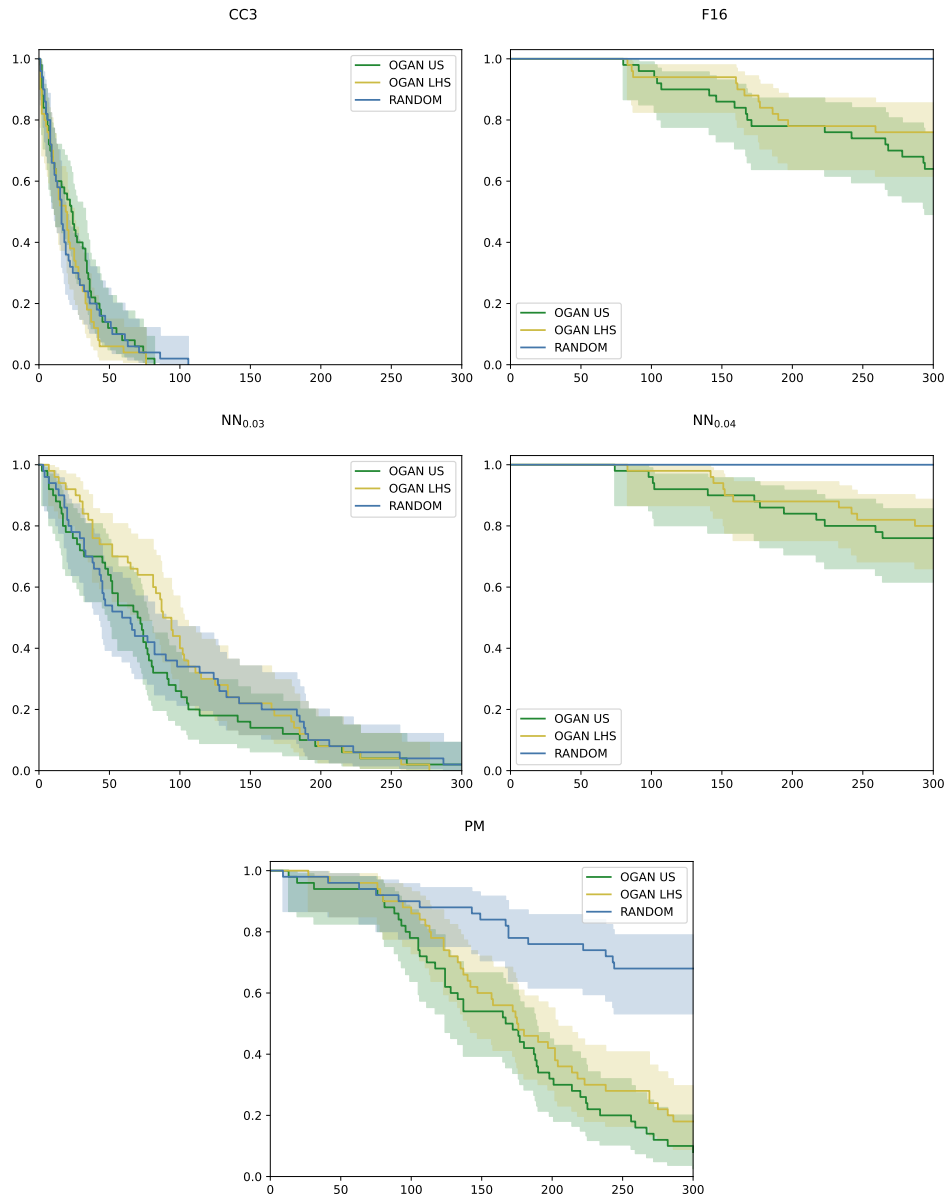


Figure 4: Figure 3 continued.

Req.	STGEM: RANDOM			STGEM: OGAN US			STGEM: OGAN LHS		
	FR	95% CI	\bar{S}	FR	95% CI	\bar{S}	FR	95% CI	\bar{S}
AFC27	0.42	[0.30, 0.57]	126.8	1.00	[1.00, 1.00]	76.8	1.00	[1.00, 1.00]	73.1
AT1 ₂₀	0.00	[0.00, 0.00]	–	0.82	[0.70, 0.91]	119.1	0.70	[0.57, 0.82]	154.8
ATX2	0.12	[0.06, 0.25]	68.2	0.48	[0.35, 0.63]	159.2	0.56	[0.43, 0.70]	144.2
AT6 _{4,35,3000}	0.50	[0.37, 0.64]	159.2	1.00	[1.00, 1.00]	88.0	1.00	[1.00, 1.00]	81.5
AT6 _{8,50,3000}	0.16	[0.08, 0.29]	123.6	1.00	[1.00, 1.00]	132.4	0.96	[0.88, 0.99]	123.3
AT6 _{20,65,3000}	0.28	[0.18, 0.43]	113.4	0.96	[0.88, 0.99]	92.3	0.98	[0.91, 1.00]	89.6
AT6 _{30,80,4500}	0.86	[0.75, 0.94]	103.1	0.88	[0.77, 0.95]	105.7	0.88	[0.77, 0.95]	110.1
AT6 _{30,50,2700}	0.04	[0.01, 0.15]	225.5	0.92	[0.82, 0.97]	120.2	0.98	[0.91, 1.00]	137.0
CC3	1.00	[1.00, 1.00]	23.5	1.00	[1.00, 1.00]	25.7	1.00	[1.00, 1.00]	21.0
CC4	0.00	[0.00, 0.00]	–	0.00	[0.00, 0.00]	–	0.00	[0.00, 0.00]	–
F16	0.00	[0.00, 0.00]	–	0.36	[0.24, 0.51]	183.3	0.24	[0.14, 0.38]	160.7
NN _{0.03}	0.86	[0.75, 0.94]	85.8	0.98	[0.91, 1.00]	76.0	1.00	[1.00, 1.00]	101.1
NN _{0.04}	0.00	[0.00, 0.00]	–	0.24	[0.14, 0.38]	168.5	0.20	[0.11, 0.34]	183.8
PM	0.32	[0.21, 0.47]	144.5	0.92	[0.82, 0.97]	155.7	0.82	[0.70, 0.91]	161.2

Table 5: Falsification results over 50 independent replicas for uniform random search, OGAN with uniform random sampling as initial random search, and OGAN with Latin hypercube sampling as initial random search for the benchmarks of Subsection 5.3.

It is immediate that OGAN consistently beats uniform random search by a large margin in effectiveness and efficiency. The only exceptions are the benchmarks AT6_{30,80,4500}, CC3, and NN_{0.03} where all three algorithms have equal performance as indicated by Figures 3, 4. This observation is supported by the fact that the corresponding logrank test p -values under the hypothesis that OGAN US and random search have identical survival functions are 0.869, 0.736, and 0.608. When comparing OGAN LHS and random search, the respective p -values are 0.984, 0.580, and 0.738. Nevertheless, OGAN always performs as well as uniform random search and typically much better.

As is evident from Table 6, OGAN US and OGAN LHS yield similar performance. Only in the benchmark AT1₂₀ is there a marked difference. Given that the performance is similar on the other benchmarks, this is likely explained by the characteristics of this benchmark, but we have not studied it further. We conclude that using LHS over uniform random sampling does not yield a marked difference in OGAN’s performance.

Answer to RQ3. OGAN performance is not affected significantly by the chosen Monte-Carlo sampling strategy.

6.3 RQ4: OGAN Computational Overhead

In order to study RQ4, we have collected the total time T to complete each replica and the time t it takes to generate a single test for both OGAN and the uniform random search algorithm. The total time T aggregates the time required to generate and execute all tests. On the other hand, the test generation time t does not include test execution time. It includes the time it takes to train the models and the time it takes to generate a new candidate test. We expect that the generation time is negligible for the uniform random search algorithm. It can be considerably larger for OGAN due to the training of neural networks. Whether or not this overhead is relevant depends on how long it takes to execute a test on the SUT. To make the execution time more concrete, we report the ratio R defined as the ratio of the total time used for execution and the

Req.	STGEM: RANDOM			STGEM: OGAN US		
	\bar{t}	\bar{T}	R	\bar{t}	\bar{T}	R
AFC27	*	444.6	1.00	0.12	192.5	0.95
AT1 ₂₀	*	142.0	1.00	1.22	286.8	0.35
ATX2	*	137.5	1.00	1.86	557.0	0.23
AT6 _{4,35,3000}	*	122.4	1.00	0.53	130.3	0.64
AT6 _{8,50,3000}	*	134.5	1.00	1.07	236.0	0.40
AT6 _{20,65,3000}	*	127.2	1.00	0.70	154.5	0.54
AT6 _{30,80,4500}	*	91.5	1.00	1.37	269.3	0.34
AT6 _{30,50,2700}	*	141.1	1.00	1.12	244.6	0.38
CC3	*	67.9	1.00	0.01	70.6	1.00
CC4	*	327.2	1.00	3.27	1348.6	0.27
F16	*	25.0	1.00	1.20	334.3	0.07
NN _{0.03}	*	122.3	1.00	0.92	188.1	0.61
NN _{0.04}	*	320.3	1.00	2.04	847.8	0.35
PM	*	126.1	1.00	1.16	291.9	0.34

Table 8: Time measurements over 50 independent replicas for uniform random search and OGAN US. We report the mean test generation time \bar{t} , the mean total time \bar{T} , and the ratio R of total execution time to the sum of total times. All times are measured in wall time and in seconds. Asterisk * indicates that the measurement was smaller than 1×10^{-4} .

total time (totals are computed over all replicas). The data is from the replicas of Subsection 6.2.

The collected time measurements are displayed in Table 8. As expected, the uniform random search algorithm spends all of its time executing tests, and its computational overhead is negligible. It is clear that OGAN has a significant computational overhead on almost all benchmarks. The time measurements for AFC27 and CC3 are low, but this is explained by the fact that often already the initial random sampling manages to find a falsifying input: the neural networks are trained only a few times, and this accounts to little overhead. It is worth remarking that on the AFC27 benchmark OGAN manages to achieve a significantly lower mean total time than the random search algorithm. We believe this is because it is very easy for the discriminator to learn from its training data what is a falsifying input. Thus OGAN gains a significant advantage.

The ratios R indicate that typically OGAN uses less than half of the time for test execution. Since we have assumed that test execution is expensive, it follows that using OGAN is even more expensive timewise. Thus if time is the main concern, then OGAN might not be the tool of choice for the selected benchmarks. However, notice that the execution time is independent of the OGAN algorithm. If the execution took several minutes, then the ratio R would be automatically very high provided that the OGAN setup is not altered. This would make OGAN a much more appealing approach. If effectiveness and efficiency are also important, as they should be, OGAN is a viable choice even when SUT execution is fast. In general, it is difficult to meaningfully compare computational overheads between algorithms that are not equally effective and efficient.

Answer to RQ4. OGAN incurs a significant computational overhead over random search on the selected benchmarks. This is mainly due to the training of neural networks. The severity of the overhead depends on the SUT execution time, which is independent of OGAN.

6.4 RQ5: OGAN Discriminator Accuracy

The OGAN discriminator \mathcal{D} functions as a surrogate model for the composition of the SUT \mathcal{M} and the robustness metric ρ . Ideally, the discriminator accurately models the mapping $x \mapsto \rho(\mathcal{M}(x))$ where x is in the input space \mathcal{I} . This is, however, not a strict requirement for successful falsification as the discussion of Subsection 2.4 merely assumes that low-robustness areas of the input space are modeled sufficiently well. In this section, we study the accuracy of the OGAN discriminators learned during the experiments of Subsection 6.2 and answer RQ5.

Consider a benchmark from Subsection 5.3. Let \mathcal{B} be a balanced validation set, obtained independently of the results of Subsection 6.2, such that, for all $i = 0, \dots, 9$, the size of the set

$$\left\{ x \in \mathcal{B} : \rho(\mathcal{M}(x)) \in \left[\frac{M}{10}i, \frac{M}{10}(i+1) \right) \right\}$$

is 25 whenever it is nonempty (nonemptiness is determined empirically based on 10000 uniformly randomly selected inputs). Here M is the empirical maximum of $\rho \circ \mathcal{M}$ computed from 10000 uniformly randomly selected inputs. For a given OGAN discriminator \mathcal{D} , we compute an accuracy score $M(\mathcal{D})$ as the mean absolute error:

$$M(\mathcal{D}) = \frac{1}{|\mathcal{B}|} \sum_{x \in \mathcal{B}} |\mathcal{D}(x) - \rho(\mathcal{M}(x))|.$$

Observe that the loss of Subsection 5.4 that was used to train the discriminators is different from the mean absolute error. We use the mean absolute error here as it is more interpretable.

Table 9 reports the means and standard errors for the accuracy scores for each benchmark from Subsection 5.3 and both OGAN variants of Subsection 6.2. The selected discriminators were the OGAN discriminators trained when the falsification tasks of Subsection 6.2 terminated. Thus a sample size of 50 discriminators was used to compute each statistic. It is evident that typically the mean absolute error is rather large especially given that the range of $\rho \circ \mathcal{M}$ is $[0, M]$. The exceptional results for the benchmark CC4 are explained by the fact that the empirical maximum 0.008 is a small number. Notice also that the benchmark CC3 is, on average, falsified by the initial random search. It follows that in this case the majority of the discriminators were never trained, and the scores mainly reflect the accuracy of a discriminator with randomly initialized weights.

We conclude that the OGAN discriminators trained with a limited budget (300 tests) are not globally accurate models, but they model the low-robustness regions well-enough since they perform better than random search as explained in Subsection 6.2. Manual inspection of several discriminators reveals that discriminator estimates are often biased in the sense that their range is much narrower than the expected range of $[0, 1]$. Since falsification nevertheless succeeds, this is not a problem: it is enough that the lower end of the discriminator range maps reasonably well to a low-robustness area of $\rho \circ \mathcal{M}$.

Answer to RQ5. The trained discriminators are not globally accurate models. However, they estimate the robustness well enough to guide OGAN towards falsifying inputs.

6.5 RQ6: The Role of Generator Sampling

In Subsection 2.4, we proposed to use the generator to augment the discriminator’s training data. Here we study the effect of this compared to using Monte-Carlo sampling independent of the generator. We do this by considering a variant of OGAN, which we call nonadaptive OGAN, and compare it to the unmodified OGAN which we call here adaptive OGAN. Otherwise we use the benchmarks and setup of Subsection 6.1.2. We consider two Monte-Carlo sampling strategies: uniform random sampling and Latin hypercube sampling. To be clear, the sampling probability P is set to 0 in adaptive OGAN.

In the nonadaptive variant, we sample two tests to be executed: test t_1 using the first branch of the if statement in the function SAMPLE_TEST of Algorithm 1 and another test t_2 using

Req.	OGAN US:		OGAN LHS:	
	Mean	SD	Mean	SD
AFC27	0.28	0.02	0.27	0.02
AT1 ₂₀	0.13	0.03	0.14	0.04
ATX2	0.21	0.01	0.21	0.01
AT6 _{4,35,3000}	0.29	0.04	0.30	0.04
AT6 _{8,50,3000}	0.29	0.03	0.30	0.03
AT6 _{20,65,3000}	0.30	0.03	0.29	0.04
AT6 _{30,80,4500}	0.21	0.01	0.21	0.01
AT6 _{30,50,2700}	0.30	0.04	0.30	0.04
CC3	0.46	0.11	0.46	0.11
CC4	0.00	0.00	0.00	0.00
F16	0.05	0.03	0.05	0.03
NN _{0.03}	0.24	0.03	0.26	0.03
NN _{0.04}	0.26	0.02	0.27	0.02
PM	0.14	0.06	0.14	0.05

Table 9: Averages and standard deviations of the mean absolute errors for the OGAN discriminators from Subsection 6.2.

the other branch. The test t_1 and its robustness are added to the discriminator’s training data whereas t_2 and its robustness are saved but not used for training purposes. After the algorithm has terminated, we report the number of executions needed for a falsification based on the tests t_2 not the tests t_1 . Essentially, the training of the discriminator is based on randomly sampled tests and the success of the falsification is determined by the tests sampled from the generator. We emphasize that we keep the execution budget the same but count the execution of the tests t_1 and t_2 as a single execution. Without this, the comparison cannot be meaningfully done. We also remark that the initial random search phase is the same in both variants.

For the benchmarks of Subsection 5.3, Table 10 reports the FRs and their 95 % confidence intervals for adaptive OGAN and nonadaptive OGAN with both uniform random sampling (US) and LHS. Each statistic is based on 50 replicas. Figures 5, 6 depict the estimated survival functions for the two variants that use LHS. The survival functions are very similar for uniform random sampling, so we omit them. Again, the benchmark CC4 is omitted. Table 7 reports the p -values of the log-rank test under the hypothesis that the number of executions required for finding a falsifying test for adaptive OGAN and nonadaptive OGAN are from the same distribution. Rejection of the hypothesis means that the two algorithms perform differently on a given benchmark. Notice that the falsification results of the adaptive OGAN match those described in Subsection 6.1.2.

From Table 10, we see that on the benchmarks AFC27, AT6_{4,35,3000}, AT6_{8,50,3000}, AT6_{20,65,3000}, AT6_{30,50,2700}, CC3, and NN both adaptive OGAN and nonadaptive OGAN have full or almost full FR without much difference between the two variants. The corresponding p -values in Table 7 are also high indicating no difference between the variants except in the case of AT6_{4,35,3000} and NN with LHS sampling. The explanation is found from Figures 5 and 6: one variant consistently falsifies faster than the other variant. The survival functions are thus different, but the difference in effectiveness is not large. If we accept the difference of FRs as an effect size, the effect size is 0.00 for both benchmarks indicating no effect.

The adaptive variant is a clear winner on the benchmarks ATX2, AT6_{30,80,4500}, and F16. On the first two benchmarks, the nonadaptive variant performs very poorly. In the case of F16, the p -values do not indicate a statistically significant difference, but the p -values are nevertheless on the smaller side. The effect sizes 0.16 (US) and 0.10 (LHS) to the favor of the adaptive variant

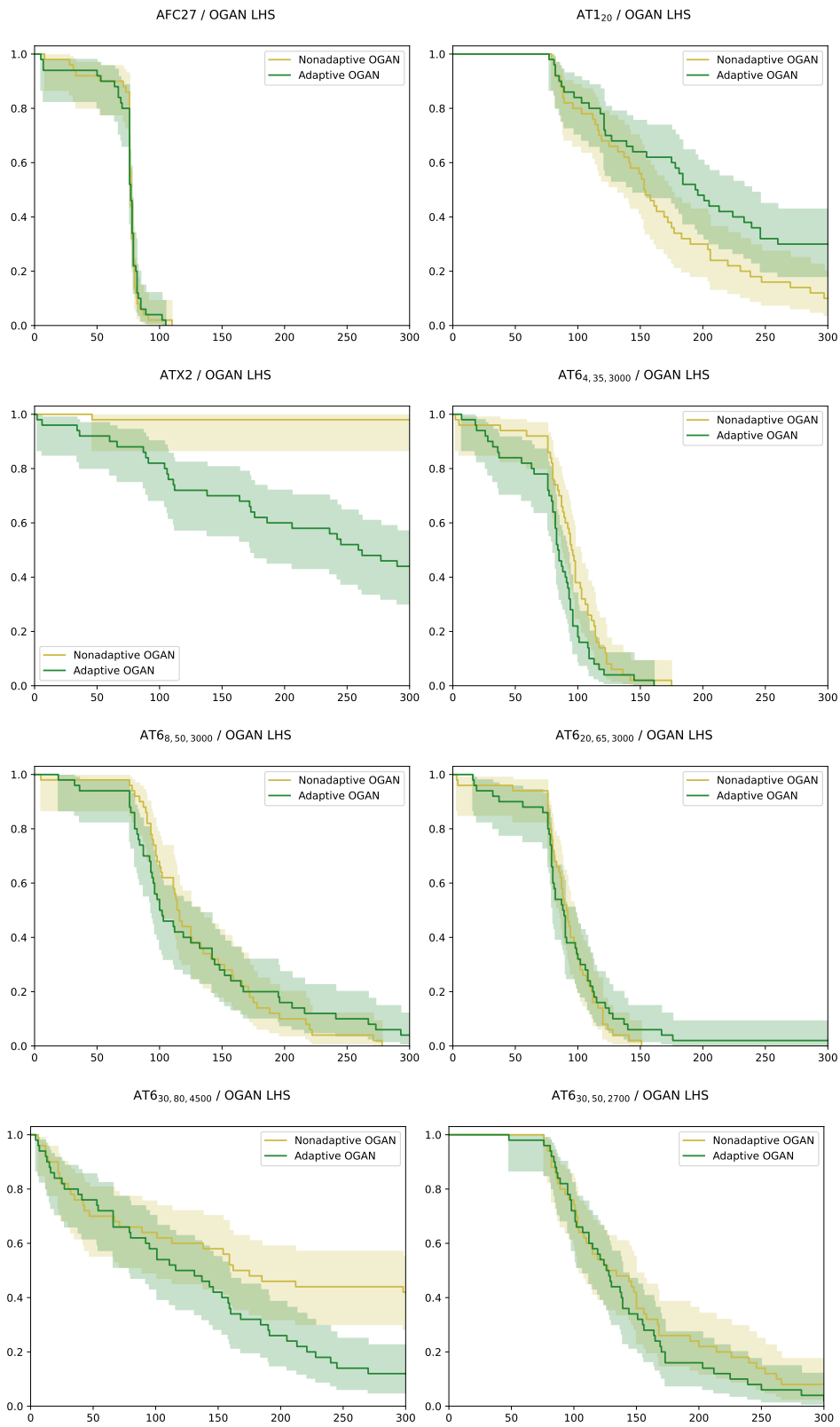


Figure 5: Survival functions for adaptive OGAN and nonadaptive OGAN using uniform random sampling for the benchmarks of Subsection 5.3.

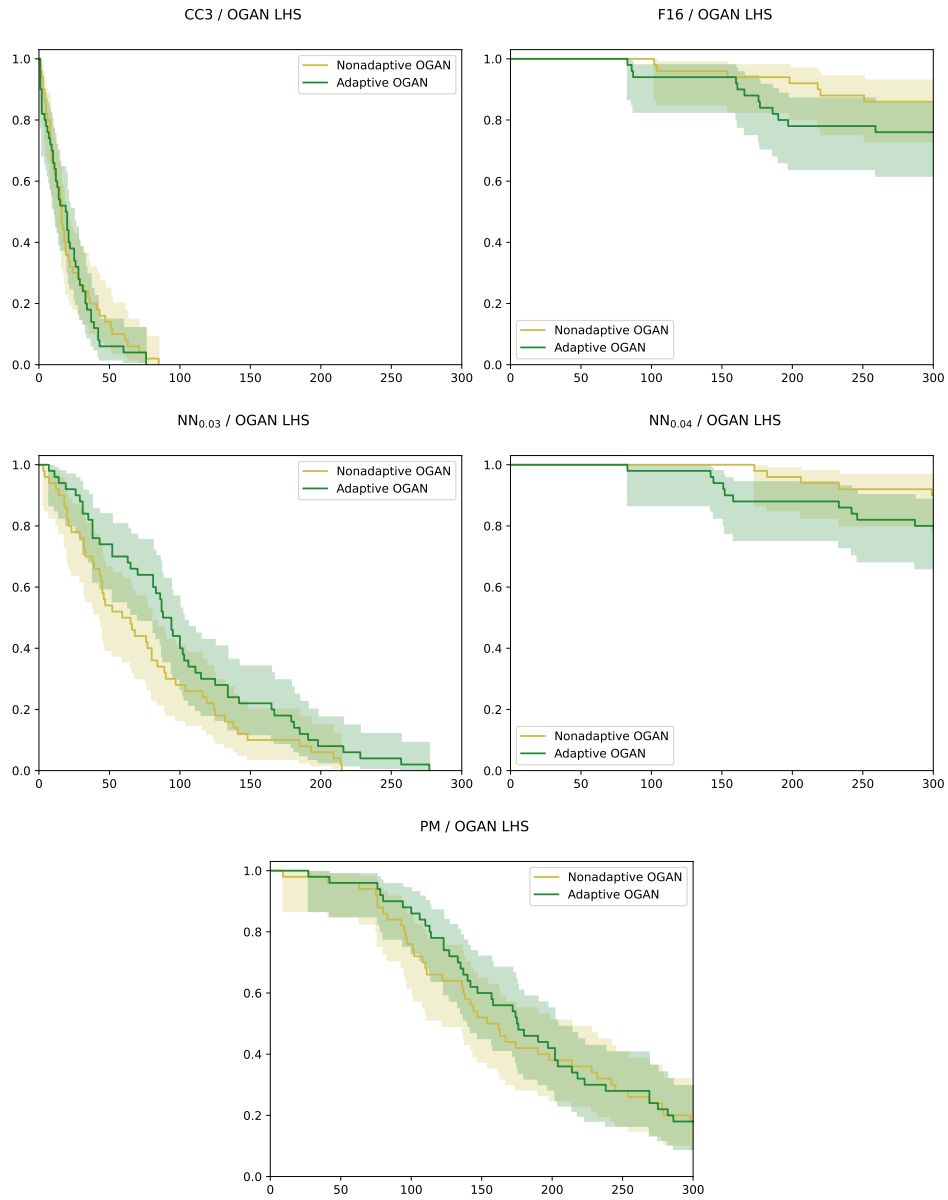


Figure 6: Figure 5 continued.

Req.	Adaptive OGAN: US		Nonadaptive OGAN: US		Adaptive OGAN: LHS		Nonadaptive OGAN: LHS	
	FR	95 % CI	FR	95 % CI	FR	95 % CI	FR	95 % CI
AFC27	1.00	[1.00, 1.00]	1.00	[1.00, 1.00]	1.00	[1.00, 1.00]	1.00	[1.00, 1.00]
AT1 ₂₀	0.82	[0.70, 0.91]	0.90	[0.80, 0.96]	0.70	[0.57, 0.82]	0.90	[0.80, 0.96]
ATX2	0.48	[0.35, 0.62]	0.04	[0.01, 0.15]	0.56	[0.43, 0.70]	0.02	[0.00, 0.13]
AT6 _{4,35,3000}	1.00	[1.00, 1.00]	1.00	[1.00, 1.00]	1.00	[1.00, 1.00]	1.00	[1.00, 1.00]
AT6 _{8,50,3000}	1.00	[1.00, 1.00]	0.96	[0.88, 0.99]	0.96	[0.88, 0.99]	1.00	[1.00, 1.00]
AT6 _{20,65,3000}	0.96	[0.88, 0.99]	1.00	[1.00, 1.00]	0.98	[0.91, 1.00]	1.00	[1.00, 1.00]
AT6 _{30,80,4500}	0.88	[0.77, 0.95]	0.54	[0.41, 0.68]	0.88	[0.77, 0.95]	0.58	[0.45, 0.72]
AT6 _{30,50,2700}	0.92	[0.82, 0.97]	0.88	[0.77, 0.95]	0.98	[0.91, 1.00]	0.92	[0.82, 0.97]
CC3	1.00	[1.00, 1.00]	1.00	[1.00, 1.00]	1.00	[1.00, 1.00]	1.00	[1.00, 1.00]
CC4	0.00	[0.00, 0.00]	0.00	[0.00, 0.00]	0.00	[0.00, 0.00]	0.00	[0.00, 0.00]
F16	0.36	[0.24, 0.51]	0.20	[0.11, 0.34]	0.24	[0.14, 0.38]	0.14	[0.07, 0.27]
NN _{0.03}	0.98	[0.91, 1.00]	0.98	[0.91, 1.00]	1.00	[1.00, 1.00]	1.00	[1.00, 1.00]
NN _{0.04}	0.24	[0.14, 0.38]	0.24	[0.14, 0.38]	0.20	[0.11, 0.34]	0.10	[0.04, 0.22]
PM	0.92	[0.82, 0.97]	0.80	[0.68, 0.89]	0.82	[0.70, 0.91]	0.82	[0.70, 0.91]

Table 10: Falsification rates and their 95% confidence intervals for adaptive OGAN and nonadaptive OGAN for the benchmarks of Subsection 5.3.

are also quite large. On the benchmarks NN_{0.04} and PM, the nonadaptive variant suffers a big loss of effectiveness but only on one of the two sampling strategies. In the case of NN_{0.04}, a part of the loss is perhaps explained by the fact that the adaptive variant with LHS is slightly worse than the adaptive variant with US. For PM, we do not observe similar associations.

The only benchmark on which the adaptive variant loses to the nonadaptive variant is AT1₂₀. The effect sizes are -0.08 (US) and -0.20 (LHS) and the corresponding p -values are 0.79 and 0.02 indicating a statistically significant difference only in the latter case.

Based on the above discussion, we answer RQ6 as follows.

Answer to RQ6. Augmenting the discriminator’s training data by adaptively sampling the generator is a good feature. Disabling adaptive sampling can decrease effectiveness drastically even to the point of being unable to find falsifying inputs. Generally, adaptive sampling has at least as good effectiveness and efficiency as nonadaptive sampling.

7 Related Work

Robustness-based falsification is a widely studied problem in the research literature [4, 7]. The friendly ARCH-COMP research competition [13, 14, 33] considers several CPS requirement falsification benchmarks that can be considered as standard in this research area.

The tools and algorithms that participated in the ARCH-COMP competitions are briefly described below; for detailed information, see the competition reports [13, 33]. The majority of the entries to the ARCH-COMP competition can be considered as general black-box optimization algorithms, but the competition also includes approaches like reinforcement-learning-based falsification [47] and falsification using parametric surrogate models [34]. See Table 2 to find out which of the tools use atomic test execution and which utilize precollected data or models.

The following tools, and OGAN, participated in ARCH COMP 2023.

- **ARISTEO** [34]. This tool builds and refines a parametric surrogate model from the ARX-2

family. The surrogate is subjected to black-box testing using the S-TaLiRo falsification tool [1] with default settings.

- **ATheNA** [18]. Under the hood, ATheNA uses S-TaLiRo and simulated annealing. The novelty of this tool is the use of custom robustness functions which combine the usual STL robustness function with a benchmark-specific robustness function provided by the user. Therefore, ATheNA makes use of some a priori knowledge about the SUT.
- **FalCAuN** [45]. This method actively learns an automaton representing the SUT and the requirement. Model checking is performed on the automaton to find a counterexample.
- **FORESEE** [48]. FORESEE is built on top of the Breach falsification tool [10], and it uses CMA-ES [22] as the optimization algorithm. The novelty of the tool is in the use QB-robustness as robustness metric.
- **NNFal**⁵. The NNFal tool assumes that there exists a pretrained neural network model for the SUT. The falsification problem can then be approached as an adversarial attack on the network. See [42] for the adversarial attack approach on which NNFal ultimately relies.
- **Ψ -TaLiRo** [43]. Ψ -TaLiRo [43] is a Python implementation of S-TaLiRo [1] with a different set of optimization algorithms. It supports the ConBO algorithm which is based on Bayesian optimization. It also supports the Part-X algorithm which estimates failure probabilities [36].

There are five tools that participated in ARCH-COMP 2021 that are not described earlier.

- **Breach** [10]. Breach is a falsification pipeline supporting various algorithms for requirement falsification. Here, Breach has been used with the global Nelder-Mead algorithm (GNM) [35] and CMA-ES [22]. Both algorithms aim to minimize a robustness metric.
- **falsify** [47]. This tool trains in advance (using the A3C algorithm) a reinforcement learning agent that attempts to build a falsifying input piece-by-piece. This requires nonatomic testing, i.e., the SUT must be observable and controllable during test execution. Moreover, the proposed method is applicable only to certain STL requirements of the form $\Box\varphi$.
- **FALSTAR** [15]. FALSTAR is a falsification pipeline. Here it is used with the adaptive Las Vegas tree search (aLVTS) algorithm. This algorithm is based on partitioning the search space into finer and finer parts based on certain probabilistic criteria. FALSTAR uses nonatomic testing to build its inputs signals a test executes.
- **S-TaLiRo** [1]. Like Breach and FALSTAR, S-TaLiRo is a falsification pipeline. In ARCH-COMP 2021, it was configured to use the SOAR optimization algorithm [32] which uses Bayesian optimization.
- **zlscheck**⁶. The zlscheck tool assumes that a benchmark has been rewritten in the Zélus programming language. This allows zlscheck to observe the system output during the simulation and to access the internals of the SUT. The robustness minimization and internal mode targeting are performed using gradient descent.

Most of the above falsification algorithms use a direct search and thus do not create a model for the robustness response of the SUT. The OGAN algorithm trains its discriminator as a surrogate model that is refined over time as more data is available. Methods based on Bayesian optimization [32, 8] are the most similar to our approach as they use and refine Gaussian process surrogates.

The OGAN algorithm is inspired by the training of generative adversarial networks, but it does not follow the traditional GAN training [21] where the discriminator is trained to distinguish between fake and real samples. The traditional approach does not fit our purposes as we lack

⁵<https://gitlab.com/Atanukundu/NNFal>

⁶<https://github.com/ismailbennani/zlscheck>

a dataset, and we need to generate the tests online. To our knowledge, there is only one other requirement falsification algorithm that uses generative models: the WOGAN algorithm [38, 39, 46]. WOGAN uses Wasserstein generative adversarial networks and, in contrast to OGAN, is designed to find multiple and diverse counterexamples for a given requirement.

Finally, we should note that there are other generative models in addition to generative adversarial networks. Recently, diffusion models have become very popular especially in image generation [9]. Diffusion models can also be used for black-box optimization [29], but we do not know of any attempt to use them for CPS requirement falsification.

8 Conclusions

We have described in detail the OGAN algorithm for robustness-based falsification. OGAN can be used to find inputs that serve as counterexamples for the safety of real-time cyber-physical systems. OGAN is based on the concept of atomic test execution, and it can be used with systems that cannot be observed or controlled during the execution of a test.

OGAN trains a generative model using of two neural networks: a generator and a discriminator. The training is performed tabula rasa without knowledge of previous execution traces. At each iteration of the algorithm, the discriminator uses the results of previously executed tests to learn the mapping from inputs to robustness values while the generator learns to map noise to inputs that the discriminator estimates to have low robustness. The generator is then sampled for an input, and the selected input is used as a test against the actual SUT. It is expected that this process eventually generates a test with actual low robustness and a counterexample for the safety of the SUT is found. To our knowledge, OGAN is the first algorithm that uses generative machine learning models for requirement falsification.

In addition to presenting the OGAN algorithm, we have proposed a novel way to transform an STL robustness metric into a scaled robustness metric taking values in the interval $[0, 1]$. Using a scaled robustness metric has the benefit that all neural network models used in the OGAN algorithm can be agnostic about the actual scales of the SUT inputs and outputs. We also believe that scaling contributes to the falsification performance as it is commonly accepted that scaling and normalization help to improve convergence in neural network training [30].

We consider that the design of OGAN is sound. The study of its Monte Carlo sampling strategy shows that while OGAN requires a source of randomness for its exploration of the input space, OGAN’s performance does not depend on the sampling method used (RQ3). Also, it is not necessary that the OGAN discriminator has high prediction accuracy; it is enough that the discriminator can direct the search towards falsifying inputs (RQ5). This indicates that OGAN is robust against minor modeling errors and prediction errors. This may be a further indication that OGAN can also perform well when the SUT is not completely deterministic. Another key element in the design of OGAN is its adaptive sampling method driven by its generator. We have designed an experiment that compares OGAN against a variant that collects training data using random sampling. We found out that the variant can perform very poorly compared to OGAN and that the adaptive sampling method is a good design choice without apparent drawbacks (RQ6).

We evaluated OGAN on several standard CPS benchmarks from the falsification track of the ARCH-COMP competition. For this, we proposed an evaluation method based on survival analysis. We believe that survival analysis has not been used for performance evaluation in the context of requirement falsification. Our opinion is that survival analysis is a useful tool as it provides both statistical tests and easily interpretable visual graphs.

In our evaluation we found that OGAN exhibits state-of-the-art CPS falsification efficiency and effectiveness (RQ1 and RQ2). OGAN has a good performance on many different benchmarks. However, due to the computational overhead introduced by OGAN (RQ4), OGAN is mainly intended for systems where testing has a significant cost (time or other resources).

Acknowledgments

We thank the organizers and participants of the falsification track of the ARCH-COMP competitions for creating a standard set of CPS falsification benchmarks with publicly available data. We thank Valentin Soloviev for fruitful discussions regarding the experiment evaluation.

This research has received funding from the ECSEL Joint Undertaking (JU) under grant agreement No 101007350. The JU receives support from the European Union’s Horizon 2021 research and innovation program and Sweden, Austria, Czech Republic, Finland, France, Italy, Spain.

References

- [1] Y. Annapureddy, C. Liu, G. Fainekos, and S. Sankaranarayanan. S-TaLiRo: A tool for temporal logic falsification for hybrid systems. In P. A. Abdulla and K. R. M. Leino, editors, *International Conference on Tools and Algorithms for the Construction and Analysis of Systems. TACAS 2011*, pages 254–257. Springer, 2011.
- [2] A. Arcuri and Lionel Briand. A hitchhiker’s guide to statistical tests for assessing randomized algorithms in software engineering. *Journal of Software: Testing, Verification and Reliability*, 24(3):219–250, 2012. doi:10.1002/stvr.1486.
- [3] M. Ayesh et al. Two simulink models with requirements for a simple controller of a pacemaker device. In *9th International Workshop on Applied Verification of Continuous and Hybrid Systems. ARCH22*, volume 90 of *EPiC Series in Computing*, pages 18–25. EasyChair, 2022. doi:10.29007/f57w.
- [4] E. Bartocci et al. Specification-based monitoring of cyber-physical systems: A survey on theory, tools and applications. In E. Bartocci and Y. Falcone, editors, *Lectures on Runtime Verification: Introductory and Advanced Topics*, volume 10457 of *Lecture Notes on Computer Science*, pages 135–175. Springer, 2018. doi:10.1007/978-3-319-75632-5_5.
- [5] E. Bartocci and Y. Falcone, editors. *Lectures on Runtime Verification - Introductory and Advanced Topics*, volume 10457 of *Lecture Notes in Computer Science*. Springer, 2018. doi:10.1007/978-3-319-75632-5.
- [6] J. J. Buckley and E. Eslami. *An Introduction to Fuzzy Logic and Fuzzy Sets*. Springer, 2002. doi:10.1007/978-3-7908-1799-7.
- [7] A. Corso, R. J. Moss, M. Koren, R. Lee, and M. J. Kochenderfer. A survey of algorithms for black-box safety validation of cyber-physical systems. *Journal of Artificial Intelligence Research*, 72:377–428, 2021. doi:10.1613/jair.1.12716.
- [8] J. V. Deshmukh, M. Horvat, X. Jin, R. Majumdar, and V. S. Prabhu. Testing cyber-physical systems through Bayesian optimization. *ACM Transactions on Embedded Computing Systems*, 16(5s):170:1–18, 2017. doi:10.1145/3126521.
- [9] P. Dhariwal and A. Nichol. Diffusion models beat GANs on image synthesis. *CoRR*, abs/2105.05233, 2021. arXiv:2105.05233.
- [10] A. Donzé. Breach, a toolbox for verification and parameter synthesis of hybrid systems. In T. Touili, B. Cook, and P. Jackson, editors, *International Conference on Computer-Aided Verification. CAV 2010*, volume 6174 of *Lecture Notes in Computer Science*, pages 167–170. Springer, 2010. doi:10.1007/978-3-642-14295-6_17.
- [11] A. Donzé and O. Maler. Robust satisfaction of temporal logic over real-valued signals. In K. Chatterjee and T. A. Henzinger, editors, *Formal Modeling and Analysis of Timed Systems. FORMATS 2010*, volume 6246 of *Lecture Notes in Computer Science*, pages 92–106. Springer, 2010. doi:10.1007/978-3-642-15297-9_9.

- [12] T. Dreossi et al. Efficient guiding strategies for testing of temporal properties of hybrid systems. In K. Havelund, G. Holzmann, and R. Joshi, editors, *NASA Formal Methods. NFM 2015*, volume 9058 of *Lecture Notes in Computer Science*, pages 127–142. Springer, 2015. doi:10.1007/978-3-319-17524-9_10.
- [13] G. Ernst et al. ARCH-COMP 2021 category report: Falsification with validation of results. In G. Frehse and M. Althoff, editors, *8th International Workshop on Applied Verification of Continuous and Hybrid Systems. ARCH21*, volume 80 of *EPiC Series in Computing*, pages 133–152. EasyChair, 2021. doi:10.29007/xw11.
- [14] G. Ernst et al. ARCH-COMP 2022 category report: Falsification with unbounded resources. In G. Frehse, M. Althoff, E. Schoitsch, and J. Guiochet, editors, *9th International Workshop on Applied Verification of Continuous and Hybrid Systems. ARCH22*, volume 90 of *EPiC Series in Computing*, pages 203–221. EasyChair, 2022. doi:10.29007/fhnk.
- [15] G. Ernst, S. Sedwards, Z. Zhang, and I. Hasuo. Falsification of hybrid systems using adaptive probabilistic search. *ACM Transactions on Modeling and Computer Simulation*, 31(3), 2021. doi:10.1145/3459605.
- [16] G. Fainekos, B. Hoxha, and S. Sankaranarayanan. Robustness of specifications and its applications to falsification, parameter mining, and runtime monitoring with S-TaLiRo. In B. Finkbeiner and L. Mariani, editors, *Runtime Verification. RV 2019*, volume 11757 of *Lecture Notes in Computer Science*, pages 27–47. Springer, 2019. doi:10.1007/978-3-030-32079-9_3.
- [17] G. Fainekos and G. J. Pappas. Robustness of temporal logic specifications for continuous-time signals. *Theoretical Computer Science*, 410:4262–4291, 2009. doi:10.1016/j.tcs.2009.06.021.
- [18] F. Formica, M. Askarpour, and C. Menghi. Search-based software testing driven by automatically generated and manually defined fitness functions. *CoRR*, abs/2207.11016, 2022. arXiv:2207.11016.
- [19] Y. Gilpin, V. Kurtz, and H. Lin. A smooth robustness measure of signal temporal logic for symbolic control. *IEEE Control Systems Letters*, 5(1):241–246, 2021. doi:10.1109/LCSYS.2020.3001875.
- [20] X. Glorot and Y. Bengio. Understanding the difficulty of training deep feedforward neural networks. In Y. W. Teh and M. Titterton, editors, *Proceedings of the Thirteenth International Conference on Artificial Intelligence and Statistics*, volume 9 of *Proceedings of Machine Learning Research*, pages 249–256, 2010. URL: <https://proceedings.mlr.press/v9/glorot10a.html>.
- [21] I. J. Goodfellow et al. Generative adversarial networks. *CoRR*, abs/1406.2661, 2014. arXiv:1406.2661.
- [22] N. Hansen. The CMA evolution strategy: A tutorial. *CoRR*, abs/1604.00772, 2016. arXiv:1604.00772.
- [23] K. He, X. Zhang, S. Ren, and J. Sun. Delving deep into rectifiers: surpassing human-level performance on ImageNet classification. In *IEEE International Conference on Computer Vision. ICCV 2015*, pages 1026–1034, 2015. doi:10.1109/ICCV.2015.123.
- [24] P. Heidlauf, A. Collins, M. Bolender, and S. Bak. Verification challenges in F-16 ground collision avoidance and other automated maneuvers. In G. Frehse, editor, *5th International Workshop on Applied Verification of Continuous and Hybrid Systems. ARCH18*, volume 54 of *EPiC Series in Computing*, pages 208–217. EasyChair, 2018. doi:10.29007/91x9.

- [25] B. Hoxha, H. Abbas, and G. Fainekos. Benchmarks for temporal logic requirements for automotive systems. In G. Frehse and M. Althoff, editors, *ARCH14–15. 1st and 2nd International Workshop on Applied Verification for Continuous and Hybrid Systems*, pages 25–30. EasyChair, 2015. doi:10.29007/xwrs.
- [26] J. Hu, J. Lygeros, and S. Sastry. Towards a theory of stochastic hybrid systems. In *Hybrid Systems: Computation and Control*, pages 160–173. Springer, 2000.
- [27] X. Jin, J. V. Deshmukh, J. Kapinski, K. Ueda, and K. Butts. Powertrain control verification benchmark. In *17th International Conference on Hybrid Systems: Computation and Control. HSCC 2014*, pages 253–262. Association for Computing Machinery, 2014. doi:10.1145/2562059.2562140.
- [28] J. D. Kalbfleisch and R. L. Prentice. *The Statistical Analysis of Failure Time Data*. Wiley, 2002. Second Edition.
- [29] S. Krishnamoorthy, S. M. Mashkaria, and A. Grover. Diffusion models for black-box optimization. *CoRR*, abs/2306.07180, 2023. arXiv:2306.07180.
- [30] Y. A. LeCun, L. Bottou, G. B. Orr, and KR. Müller. Efficient backprop. In *Neural Networks: Tricks of the Trade*, volume 7700 of *Lecture Notes in Computer Science*, pages 9–48. Springer, 2012. doi:10.1007/978-3-642-35289-8_3.
- [31] O. Maler and D. Nickovic. Monitoring temporal properties of continuous signals. In Y. Lakhnech and S. Yovine, editors, *Formal Techniques, Modelling and Analysis of Timed and Fault-Tolerant Systems. FORMATS 2004*, volume 3253 of *Lecture Notes in Computer Science*, pages 152–166. Springer, 2004. doi:10.1007/978-3-540-30206-3_12.
- [32] L. Mathesen, G. Pedrielli, S. H. Ng, and Z. B. Zabinsky. Stochastic optimization with adaptive restart: A framework for integrated local and global learning. *Journal of Global Optimization*, 79:87–110, 2021. doi:10.1007/s10898-020-00937-5.
- [33] C. Menghi et al. ARCH-COMP 2023 category report: Falsification. In G. Frehse and M. Althoff, editors, *10th International Workshop on Applied Verification of Continuous and Hybrid Systems. ARCH23*, volume 96 of *EPiC Series in Computing*, pages 151–169, 2023. doi:10.29007/6nqs.
- [34] C. Menghi, S. Nejati, L. C. Briand, and Y. Isasi Parache. Approximation-refinement testing of compute-intensive cyber-physical models: An approach based on system identification. In G. Rothermel and D.-H. Bae, editors, *ICSE '20: 42nd International Conference on Software Engineering*, pages 372–384. ACM, 2020. doi:10.1145/3377811.3380370.
- [35] J. A. Nelder and R. Mead. A simplex method for function minimization. *The Computer Journal*, 7(4):308–313, 1965. doi:10.1093/comjnl/7.4.308.
- [36] G. Pedrielli et al. Part-X: A family of stochastic algorithms for search-based test generation with probabilistic guarantees. *CoRR*, abs/2110.10729, 2021. arXiv:2110.10729.
- [37] J. Peltomäki and I. Porres. Falsification of multiple requirements for cyber-physical systems using online generative adversarial networks and multi-armed bandits. In *IEEE International Conference on Software Testing, Verification and Validation Workshops. ICSTW 2021*, 2021. doi:10.1109/ICSTW55395.2022.00018.
- [38] J. Peltomäki, F. Spencer, and I. Porres. Wasserstein generative adversarial networks for online test generation for cyber physical systems. In *15th IEEE/ACM International Workshop on Search-Based Software Testing. SBST 2022*, page 1–5, 2022. doi:10.1145/3526072.3527522.

- [39] J. Peltomäki, F. Spencer, and I. Porres. WOGAN at the SBST 2022 CPS tool competition. In *15th IEEE/ACM International Workshop on Search-Based Software Testing. SBST 2022*, pages 53–54, 2022. doi:10.1145/3526072.3527535.
- [40] I. Porres, H. Rexha, and S. Lafond. Online GANs for automatic performance testing. In *IEEE International Conference on Software Testing, Verification and Validation Workshops. ICSTW 2021*, pages 95–100, 2021. doi:10.1109/ICSTW52544.2021.00027.
- [41] J. Shi, J. Wan, H. Yan, and H. Suo. A survey of cyber-physical systems. In *2011 International Conference on Wireless Communications & Signal Processing. WCSP 2011*, pages 1–6. IEEE, 2011. doi:10.1109/WCSP.2011.6096958.
- [42] D. Shriver, S. Elbaum, and M. B. Dwyer. Reducing DNN properties to enable falsification with adversarial attacks. In *IEEE/ACM 43rd International Conference on Software Engineering. ICSE 2021*, pages 275–287, 2021. doi:10.1109/ICSE43902.2021.00036.
- [43] Q. Thibeault, J. Anderson, A. Chandratre, G. Pedrielli, and G. Fainekos. PSY-TaLiRo: A Python toolbox for search-based test generation for cyber-physical systems. In A. L. Lafuente and A. Mavridou, editors, *Formal Methods for Industrial Critical Systems. FMICS 2021*, volume 12863 of *Lecture Notes in Computer Science*. Springer, 2021. doi:10.1007/978-3-030-85248-1_15.
- [44] P. Varnai and D. V. Dimarogonas. On robustness metrics for learning STL tasks. In *American Control Conference. ACC 2020*, pages 5394–5399, 2020. doi:10.23919/ACC45564.2020.9147692.
- [45] M. Waga. Falsification of cyber-physical systems with robustness-guided black-box checking. In *Proceedings of the 23rd International Conference on Hybrid Systems: Computation and Control*. ACM, 2020. doi:10.1145/3365365.3382193.
- [46] J. Winsten and I. Porres. WOGAN at the SBFT 2023 CPS tool competition - Cyber-physical systems track. In *16th IEEE/ACM International Workshop on Search-Based and Fuzz Testing. SBFT 2023*, pages 43–44, 2023. doi:10.1109/SBFT59156.2023.00009.
- [47] Y. Yoriyuki, S. Liu, T. Akazaki, Y. Yihai, and J. Hao. Falsification of cyber-physical systems using deep reinforcement learning. *IEEE Transactions on Software Engineering*, 47(12):2823–2840, 2021. doi:10.1109/TSE.2020.2969178.
- [48] Z. Zhang et al. Effective hybrid system falsification using Monte Carlo tree search guided by QB-robustness. In A. Silva and K. R. M. Leino, editors, *Computer Aided Verification. CAV 2021*, volume 12759 of *Lecture Notes in Computer Science*, pages 595–618. Springer, 2021. doi:10.1007/978-3-030-81685-8_29.